Integrating canopy dynamics, soil moisture, and soil physical properties to improve irrigation
scheduling in turfgrass systems

by

Don Wesley Dyer

B.S., Mississippi State University, 2014
M.S., Texas A&M University, 2017

AN ABSTRACT OF A DISSERTATION

submitted in partial fulfillment of the requirements for the degree

DOCTOR OF PHILOSOPHY

Department of Horticulture and Natural Resources
College of Agriculture

KANSAS STATE UNIVERSITY
Manhattan, Kansas

2022

Abstract

This dissertation explores some components of the soil water balance in turfgrass systems that remain poorly understood. Specifically, rainfall interception of the turfgrass canopy and the canopy response to soil moisture deficits. Two research studies were conducted at Kansas State University at the Rocky Ford Turfgrass Research Center, Manhattan, KS.

The first research study (Chapter 1) investigated the magnitude of canopy interception and the role that meteorological conditions and plant canopy characteristics play in turfgrass systems. Canopy interception has largely been ignored in turfgrass irrigation scheduling programs and the magnitude of interception effects remains unknown. Canopy interception of two common turfgrass species, zoysiagrass (*Zoysia japonica* L.) and creeping bentgrass (*Agrostis stolonifera* L.), was measured during various precipitation events in the fall of 2019 and spring of 2020. Canopy throughfall amount resulted in a strong ($r = 0.98$) positive linear relationship with precipitation total. On average, zoysiagrass and creeping bentgrass canopies intercepted a minimum amount of 5 mm before throughfall occurs. This indicates that no precipitation reaches the soil surface for precipitation events < 5 mm. Nearly 60% of the contiguous United States could result in annual precipitation interception of 50% within a turfgrass canopy. This study provides detailed insights to understanding the interception dynamics in turfgrass and highlights the inefficient nature of small precipitation and irrigation events in turfgrass systems.

The second research study (Chapter 2) was conducted throughout the 2019 and 2020 growing season which focused on integrating soil moisture, canopy information, and forecasted precipitation to guide our water management decisions in 'Meyer' zoysiagrass (*Zoysia japonica* L.). We discovered that incorporating soil moisture, plant canopy conditions, and forecasted

precipitation into a decision tree resulted in water savings of 81% in 2020 and 66% in 2019 compared to a traditional fixed-amount irrigation scheduling. The decision tree is simple decision-support tool that enhanced our ability to identify and apply irrigation at the most opportune time without sacrificing turfgrass quality.

Integrating canopy dynamics, soil moisture, and soil physical properties to improve irrigation
scheduling in turfgrass systems

by

Don Wesley Dyer

B.S., Mississippi State University, 2014
M.S., Texas A&M University, 2017

A DISSERTATION

submitted in partial fulfillment of the requirements for the degree

DOCTOR OF PHILOSOPHY

Department of Horticulture and Natural Resources
College of Agriculture

KANSAS STATE UNIVERSITY
Manhattan, Kansas

2022

Approved by:

Major Professor
Dale Bremer

Copyright

Abstract

This dissertation explores some components of the soil water balance in turfgrass systems that remain poorly understood. Specifically, rainfall interception of the turfgrass canopy and the canopy response to soil moisture deficits. Two research studies were conducted at Kansas State University at the Rocky Ford Turfgrass Research Center, Manhattan, KS.

The first research study (Chapter 1) investigated the magnitude of canopy interception and the role that meteorological conditions and plant canopy characteristics play in turfgrass systems. Canopy interception has largely been ignored in turfgrass irrigation scheduling programs and the magnitude of interception effects remains unknown. Canopy interception of two common turfgrass species, zoysiagrass (Z*oysia japonica* L.) and creeping bentgrass (*Agrostis stolonifera* L.), was measured during various precipitation events in the fall of 2019 and spring of 2020. Canopy throughfall amount resulted in a strong ($r = 0.98$) positive linear relationship with precipitation total. On average, zoysiagrass and creeping bentgrass canopies intercepted a minimum amount of 5 mm before throughfall occurs. This indicates that no precipitation reaches the soil surface for precipitation events < 5 mm. Nearly 60% of the contiguous United States could result in annual precipitation interception of 50% within a turfgrass canopy. This study provides detailed insights to understanding the interception dynamics in turfgrass and highlights the inefficient nature of small precipitation and irrigation events in turfgrass systems.

The second research study (Chapter 2) was conducted throughout the 2019 and 2020 growing season which focused on integrating soil moisture, canopy information, and forecasted precipitation to guide our water management decisions in 'Meyer' zoysiagrass (*Zoysia japonica*

L.). We discovered that incorporating soil moisture, plant canopy conditions, and forecasted precipitation into a decision tree resulted in water savings of 81% in 2020 and 66% in 2019 compared to a traditional fixed-amount irrigation scheduling. The decision tree is simple decision-support tool that enhanced our ability to identify and apply irrigation at the most opportune time without sacrificing turfgrass quality.

Table of Contents

List of Figures

List of Tables

Acknowledgements

I would like to thank my major professor Dr. Dale Bremer and my committee members Dr. Andres Patrignani, Dr. Catherine Lavis, and Dr. Jack Fry for their support and guidance throughout my graduate school research and studies. I would also like to thank the team at Rocky Ford Turfgrass Research Center, Cliff Dipman, Dr. Jared Hoyle, Stew Hanson, and Wes Howe. Much appreciation to the United States Golf Association, Toro Company, Irrigation Innovation Consortium and Kansas Turfgrass Foundation for supplying the funding to complete my research. Thank you to the faculty, staff, and fellow graduate students in the Department of Horticulture and Natural Resources and Department of Agronomy for their support and memories throughout my time at Kansas State University.

Chapter 1 - Canopy Interception and Throughfall of Turfgrass

Abstract

Turfgrass management relies on frequent watering events from natural precipitation or irrigation. However, most irrigation scheduling strategies in turfgrass ignore the magnitude of canopy interception. Interception is the process by which precipitation or irrigation water is intercepted by and evaporated from plant canopies or plant residue. The objective of this study was to quantify the magnitude of precipitation interception and throughfall in 'Meyer' zoysiagrass (Zoysia japonica L.) and '007' creeping bentgrass (*Agrostis stolonifera* L.). We used a new method consisting of co-located pluviometers with and without circular turfgrass patches to measure interception and throughfall. The resulting dataset includes 15 storms and 25 individual rainfall events ranging in precipitation totals from 0.3 mm to 42.4 mm throughout the research study. Throughfall amount resulted in a strong ($r = 0.98$) positive linear relationship with precipitation totals. On average, zoysiagrass and creeping bentgrass canopies intercepted a minimum of 4.4 mm before throughfall occurred. This indicates that, on average, no precipitation reaches the soil surface for precipitation events <4.4 mm. After the point of throughfall, 16% of each additional millimeter of precipitation or irrigation is lost due to interception. Nearly, 45% of the area of the contiguous U.S. could result in >50% of the annual precipitation being intercepted by canopies of zoysiagrass and bentgrass. This study provides detailed insights to understanding the interception dynamics in turfgrass and highlights the inefficient nature of small precipitation and irrigation events in turfgrass systems.

Introduction

In the United States, there are more than 12.5 million hectares of irrigated turfgrass (Morris, 2003). Golf courses alone account for 600,000 hectares of turf that use approximately use 2.2 km^3 of water per year (Throssell et al., 2009; EIFG, 2015). Turfgrass plays an important role in recreational spaces, sport fields, and landscaping both for aesthetic purposes and to prevent soil erosion. Inevitably, the shallow (i.e., <30 cm) root system usually makes turfgrass vulnerable to soil water deficits, thus, irrigation is typically an integral component of turfgrass management. To better guide in-season irrigation decisions, such as irrigation amounts and frequencies, irrigation scheduling in turfgrass requires accurate knowledge of the components of the soil water balance (Beard, 2001). While traditional irrigation scheduling involves fixed watering amounts and frequencies, improved irrigation decisions aimed at conserving water resources typically integrate meteorological and soil moisture information to assess the ability of turfgrass to cope with the atmospheric demand given the available rootzone soil water capacity (Throssell et al., 2009). However, a component of the soil water balance that is often neglected in irrigation prescriptions is the magnitude of both natural precipitation and irrigation interception by the turfgrass canopy, which can reduce the amount of precipitation and irrigation water reaching the rootzone.

Interception can be defined as precipitation or irrigation water that is prevented from reaching the soil surface by plant canopies or surface litter. Intercepted droplets can remain on the surface of leaves, stems, and litter, and then evaporate into the atmosphere during and after precipitation events (Burgy and Pomeroy, 1958; Ochsner, 2022). As a result, interception is often considered a loss in the soil water balance (Savenije 2004; Dunkerley, 2013). In formal terms, interception can be defined as (Shachnovich et al., 2006):

$$I = P - TF \qquad \text{[Eq. 1]}$$

where I represents canopy and litter interception (mm), P is precipitation (mm), and TF is

throughfall (mm). Throughfall is defined as the amount of precipitation or irrigation water that

passes through the canopy. For clarity, in this study we limit the use of the term "precipitation"

to denote liquid precipitation. In trees and shrubs there is often an additional term for stemflow,

which is the water that flows down along branches and the main stem. Unlike trees and shrubs,

turfgrass systems are uniquely characterized by a dense plant canopy that can propagate by

stolons and/or rhizomes. Thus, mature turfgrass canopies typically develop a thatch layer of

intermingled dead and living material between the actively growing canopy and the soil surface

that can restrict and hold precipitation and irrigation water (Taylor et al., 1982; Beard, 2002). For

instance, previous studies suggested that creeping bentgrass (*Agrostis stolonifera* L.) could retain

an amount of water equivalent to 50% of the thickness of the thatch layer (Zimmerman, 1973).

Thus, in this study we use the term throughfall to denote the additive combination of both

throughfall and stemflow.

Previous studies have extensively investigated canopy interception in land covers other

than turfgrass. For example, a forage sorghum (*Sorghum bicolor* L. Moench) canopy in a humid

subtropical climate in Oklahoma, US intercepted 27-45% of the growing season rainfall (Yimam

et al., 2015). In a tallgrass prairie dominated by big bluestem (*Andropogon gerardii*), little

bluestem (*Schizachyrium scoparium*), and Indiangrass (*Sorghastrum nutans*) in the Flint Hills

region in Kansas, US, mean canopy interception throughout a two-year study accounted for 38%

of annual rainfall (Gilliam et al., 1987). A study in a coastal redwood (*Sequoia sempervirens*)

and Douglas-fir (*Pseudotsuga menziesii*) forest in northwest California, US revealed that about

22% of the annual precipitation is evaporated from the foliage and stems (Reid and Lewis,

2009). Therefore, canopy interception can play an important role in the fraction of annual precipitation that reaches the soil surface. Across most interception studies, the amount of canopy interception is related to plant canopy characteristics such as leaf area index and biomass, and meteorological factors such as rainfall amount, duration, intensity, and atmospheric evaporative demand. While considerable research has been conducted to show the impact of canopy interception in other land covers, to our knowledge no prior study has quantified the magnitude of canopy interception and throughfall in turfgrass. Unfolding this unknown component of the soil water balance could be a key element for a more efficient use of water turfgrass systems. The objective of this study was to quantify the magnitude of precipitation interception and the timing of canopy throughfall in 'Meyer' zoysiagrass (*Zoysia japonica* Steud.) and '007' creeping bentgrass using a new method consisting of co-located pluviometers.

Materials and Methods

The study was conducted at the Rocky Ford Turfgrass Research Center near Manhattan, Kansas (39°13'59.628" N, 96°34'30.612" W, 315 m a.s.l.) during September and October 2019 and from March to June 2020. The study site is characterized by an average annual temperature of 13.4 °C and an average annual rainfall of 895 mm that is concentrated during the late spring and summer months. The site belongs to the Dfa Köppen-Geiger climate classification, which is characterized by humid continental hot summers with year-round precipitation (Peel, 2007).

Throughfall and precipitation interception were measured simultaneously using a new approach consisting of co-located pluviometers with and without circular turfgrass patches inserted into the pluviometer funnel. A few hours before a storm, turfgrass patches of zoysiagrass and creeping bentgrass were cut, cleaned from debris, and then placed inside the pluviometer

4

funnel that had an opening with a diameter of 24.5 cm (Figure 1.1 A-C). The turfgrass patch encompassed the canopy leaves and the thatch layer. The turfgrass heights were maintained at 16 mm in the zoysiagrass and 12.7 mm in the bentgrass to mimic golf course fairway heights. The thickness of the patch was determined by placing the turfgrass patch between a benchtop and a rigid disk that had the same area of the patch with a mass of 1 kg on top of it. This procedure allowed us to consistently measure the thickness of all patches. At the end of each storm, canopy storage capacity was determined by completely submerging each patch in a bucket with water for 5 minutes and then allowed to drip for 1 minute on a rack before recording the mass representing the maximum storage capacity of the patch. Then, patches were oven-dried at 105 °C for 48 hours to determine the dry mass of the patch. For this experiment we used a total of nine pluviometers grouped in triplets to ensure replication of the experiment (Figure 1.1D). Each triplet had one open pluviometer (model TE525MM, Texas Electronics Inc.), one pluviometer covered with a patch of zoysiagrass, and one pluviometer covered with a patch of bentgrass (Figure 1.1C and D). Each pluviometer triplet was mounted on a pole at 1.2-meter above the ground. This height was an arbitrary, but practical choice to ensure turfgrass patches were correctly placed before a storm. All pluviometers were calibrated following the manufacturer's recommendation using a Mariotte's bottle dispensing water at a rate of 473 ml of water in 45 minutes. All sensors met the factory requirement of 100 ± 3 tips for this amount of water. In addition to precipitation, relative humidity and air temperature were monitored using a sensor (model CS215, Campbell Scientific) mounted at a height of 1.2 m. For storms in 2020, changes in soil water storage were monitored using soil moisture sensors (model CS655, Campbell Scientific) installed vertically (0-12 cm depth) in adjacent areas of bare soil and zoysiagrass. A datalogger (model CR1000, Campbell Scientific) was programmed to record all variables at one-

minute intervals, which allowed for detailed information of precipitation and throughfall measurements.

In the data analysis stage, we used a minimum inter-event time (MIT) criterion of one hour without measurable rainfall in the open pluviometers to identify individual rainfall events within a given storm (Dunkerley, 2008 and 2015). This criterion was selected to differentiate intra-storm precipitation events while still capturing low intensity precipitation events as a single event. The Python programming language was utilized to read and process the 1-minute data and identify the individual precipitation events using the selected MIT. Time series for each gauge with the same patch treatment were averaged.

Results and Discussion

During the study period we captured a total of 15 storms and 25 individual precipitation events. Canopy throughfall and interception were measured for all storms in zoysiagrass and for ten out of the 15 storms in bentgrass (Table 1), using a total of 75 different turfgrass patches. Storm precipitation totals ranged from 0.4 mm to 42.4 mm (Table 1), values that are similar to the 1st percentile (i.e., 0.25 mm d^{-1}) and 99th percentile (i.e., 57 mm d^{-1}) estimated from daily precipitation records for the 2010-2020 period for the Manhattan station of the Kansas Mesonet (Patrignani et al., 2020), which is located 2.7 km from the experimental site. Among the three open pluviometers, the average difference between the lowest and highest recorded precipitation total for all precipitation events was typically 0.5 mm and the coefficient of variation was 1.8%. The storm with the largest number of individual precipitation events occurred on 1 October 2019 (storm 3), totaling four events. The longest duration for a single precipitation event lasted 16.1 hours (storm 5a) and the shortest precipitation event lasted only 23 minutes (storm 12a). The highest maximum rainfall intensity of 97 mm h^{-1} was recorded at the minute level for a storm on

6

22 September 2019 (storm 1a). Thus, our study covered a wide range of precipitation durations,

amounts, and intensities typical for the central U.S. Great Plains (Lee et al., 2017).

Considering the total precipitation for all storms measured for each turfgrass, canopy

interception losses accounted for 34% (73 out of 214 mm) in zoysiagrass and 47% (39 out of 84

mm) in bentgrass (Table 1). The relationship between gross precipitation and throughfall amount

resulted in a strong positive linear correlation ($r = 0.98$), with an *x*-intercept of 4.4 mm (95% CI

[3.6, 5.3]), and a slope of 0.84 ($P<0.001$) (Figure 1.2). In this context, the *x*-intercept represents

the cumulative precipitation at the time throughfall (I_{tf}). The slope of this relationship represents

the precipitation losses due to interception after the point of throughfall. So, for zoysiagrass and

bentgrass, only 84% of each additional millimeter of precipitation after the point of throughfall

reaches the soil surface (Figure 1.2). Precipitation was completely intercepted by the turfgrass

patches in five out of the 15 storms (Table 1). This is significant because the long-term median

daily precipitation total for the study region is only 2.8 mm d^{-1} and only about 43% of the daily

precipitation events at the study site are >4.4 mm. The interception at the point of throughfall

found in this study for zoysiagrass and bentgrass was about 4 times larger than the I_{tf} of 1.61

mm found for a Spruce (*Picea crassifolia* Kom.) forest in the semiarid mountain regions of

China using 60 throughfall collectors (He et al., 2014). Our results are also slightly higher than

the reported I_{tf} values of 3.9 mm for a mature tallgrass prairie grasses and 3.4 mm for a close

stand of Redcedar (*Juniperus virginiana* L.) trees in central Oklahoma (Zou et al. 2015). A

mesoscale study in the region found that soil moisture sensors installed at 5 cm depth under

natural grassland vegetation typically respond to precipitation events >7.6 mm (Parker and

Patrignani, 2021), further indicating that our value of 4.4 mm is reasonable for this region. The

slope of the precipitation-throughfall relationship found in our study also agrees well with

previous studies in other land covers. For instance, the relationship between gross precipitation and throughfall in a matorral community in northeastern Mexico resulted in $r = 0.99$ and a slope of 85% (Carlyle-Moses, 2004).

The *x*-intercept and the slope of the relationship between gross precipitation and throughfall are of practical relevance to scientists and practitioners alike. Based on the findings reported in Figure 1.2, the daily interception amount could be approximated as follows:

$$I = P \qquad\qquad \text{for } P \leq I_{tf} \qquad \text{[Eq. 2]}$$

$$I = I_{tf} + 0.16\big(P - I_{tf}\big) \qquad \text{for } P > I_{tf} \qquad \text{[Eq. 3]}$$

where I_{tf} is the cumulative precipitation at the time throughfall begins and 0.16 (i.e., $1 - 0.84$) is the interception loss after throughfall (Figure 1.2). This relationship should provide a good first-order approximation for estimating the interception loss in zoysiagrass and creeping bentgrass mowed at standard heights for precipitation events up to ~45 mm d^{-1}. Further research is required to estimate whether the I_{tf} and slope found in this study can be used to estimate interception in other turfgrass canopies and other regions.

To illustrate the impact of precipitation pulses and antecedent wetting events on canopy interception and throughfall, we compared two storms that resulted in similar precipitation amount, but that had contrasting duration and number of intra-storm precipitation events (Figure 1.3). The first storm (storm 14 in Table 1) occurred on 22 May 2020 and consisted of only one precipitation event totaling 13.2 mm over the period of 141 minutes (Figure 1.3A). During storm 14, the point of throughfall occurred in the zoysiagrass canopy after 3.5 mm and in bentgrass canopy after 4.0 mm of precipitation. The total interception amount for zoysiagrass was 4.6 mm and for bentgrass was 5 mm (Table 1, Figure 1.3B). The zoysiagrass canopy intercepted 35% and the bentgrass canopy intercepted 38% of the precipitation in storm 14. On the other hand, the

8

second storm (storm 10 in Table 1) that occurred on 16 April 2020 had three intra-storm

precipitation events and lasted a total of 18.5 hours (Figure 1.3C). In this storm, the first

precipitation event with an amount of 3.9 mm was completely intercepted by both turfgrass

patches. Throughfall eventually occurred during the second precipitation event, when the

cumulative precipitation reached 5.8 mm in the zoysiagrass canopy and 6.1 mm in the bentgrass

canopy. The first, second, and third precipitation events within the zoysiagrass canopy

intercepted 100%, 29% and 37% of the precipitation and the bentgrass intercepted 100%, 47%,

and 47% for each event during the storm, respectively. This decreasing interception percentage

illustrates that the canopy interception capacity is highest at the start of a rainfall event and

decreases with precipitation (Sheng and Cai, 2019). However, during rainless break periods

water stored in the canopy can be lost to evaporation allowing the plant canopy to partially dry

and restore some of its water storage capacity (Dunkerley 2000). Considering the precipitation

total for in storm 10, the zoysiagrass canopy intercepted 54% and the bentgrass canopy

intercepted 65% of the precipitation (Figure 1.3B and D).

Detailed inspection of individual precipitation events using time series similar to those in

Figure 1.3 revealed that canopy interception in turfgrass canopies had three well-defined stages.

The first stage was characterized by complete precipitation interception by the canopy. During

the first stage, droplets from precipitation and splashing can remain on top of leaves, stems, and

litter, be evaporated, or be absorbed by plant tissue and organic material. The magnitude of each

of these processes is likely dictated by the nature of the canopy and thatch layer, precipitation

intensity, and the atmospheric demand during the precipitation event. The second stage was

characterized by both throughfall and canopy interception, although the evaporation rate may be

minor compared to throughfall amount due to the typically low (~0.1 kPa) vapor pressure deficit

during rainfall events in this region (Parker and Patrignani, 2021). The second stage exhibited a well-defined starting point (i.e., the point of throughfall, I_{tf}) at which the canopy can no longer intercept all the precipitation, and therefore, additional water droplets move through the canopy and the thatch layer. The third stage consisted of the drying of the canopy after the precipitation has ceased, which includes some dripping and evaporation. Figure 1.3A and C show the timing of the third stage either at the end of a storm with a single rainfall event (Figure 1.3A) or during rainless periods in storms with multiple precipitation events (Figure 1.3C), which appear in a recurring cycle (Figure 1.3D).

The interception stages identified in our study are similar to those identified in a prior study investigating canopy interception of forest canopies (Gash, 1979), which were defined as: 1) a wetting phase as rainfall reaches the plant canopy, 2) a saturation phase as the plant canopy reaches its maximum water storage capacity, and 3) a drying phase after precipitation has ceased. Some of the main differences between the stages identified by Gash (1979) and our study are evident in the second stage, in which the cumulative precipitation at the time of throughfall was nearly half of the measured interception storage capacity (S) using the submersion method. For instance, the zoysiagrass patches averaged $S = 8.9$ mm (SD = 1.3) and the bentgrass patches averaged $S = 9.1$ mm (SD = 1.4) (Table 2). The average interception at the point of throughfall was ~44% of the storage capacity for the zoysiagrass and ~50% for the bentgrass, thus illustrating throughfall occurs much earlier than the saturation point of the turfgrass canopy. Our findings indicate that at the point of throughfall, the amount of water held in the canopy does not necessarily match the storage capacity of the patch. The assumption of a "saturation phase" proposed by Gash (1979) does not seem to apply in turfgrass.

The method used in this experiment to quantify canopy interception and throughfall does not allow for measurements of the evaporation rate from the turfgrass canopy during the third stage after precipitation has ceased. A previous study aimed at measuring canopy interception and forest floor evaporation in a beech (*Fagus Sylvatica* L.) forest in Luxembourg resolved this problem by stacking and weighing two aluminum basins with strain gauges, so that the evaporation rate of the precipitation interpreted by the forest floor could be measured when the event ceased (Gerrits et al., 2007; Tsiko et al., 2012). So, in the context of turfgrass patches, it may be possible to place a tipping-bucket pluviometer on top of a logging scale to track the rate of canopy evaporation during the storm and during the third stage of the process.

Furthermore, for a selected set of precipitation events, we investigated the impact of canopy interception by monitoring the change in soil water storage from 0-12 cm using soil moisture sensors. For instance, during a 13.3 mm rainfall event (storm 14a), soil water storage rapidly increased in a no canopy cover (Figure 1.4A). However, under the zoysiagrass canopy cover the increase in soil water storage was much slower and delayed. By the end of the rainfall event, soil water storage was 8.8 mm less under the zoysiagrass canopy than in the bare soil area. This further illustrates the impact that canopy interception has on near-surface soil moisture conditions and the soil water balance of shallow rooted plants, like turfgrass.

After the rainfall ceased, soil water storage decreased in the bare soil area with no canopy cover (Figure 1.4A), which was likely a result of multiple factors. First, the bare soil surface was directly exposed to solar radiation, which undoubtedly altered its energy balance and resulted in higher evaporation and faster drying rates than in the soils shaded by the zoysiagrass canopy (Bremer and Ham, 1999; Bremer et al., 2001). Increasing vapor pressure deficit (atmospheric drying power) after the rainfall also increased evaporation rates (Figure 1.4B), contributing to the

11

faster drying (change in soil water storage) of bare soils compared with soils under the zoysiagrass. Finally, decreasing soil water storage in bare soils after the rainfall may have been caused in part by soil moisture redistribution to deeper soil layers (i.e., drainage).

Conversely, immediately after rainfall, the change in soil water storage was very slow in soils under the zoysiagrass canopy (Figure 1.4A). This was likely because evaporation in the zoysiagrass area was (initially) primarily from the wet canopy/thatch layer and not from the soil. This low evaporation from soils after rainfall is a positive aspect of having a turfgrass cover.

A better understanding of canopy interception can also be used to improve the estimation of other processes of the soil water balance, like runoff. For instance, in hydrology, the initial abstraction (I_a) is a term used to describe precipitation storage prior to the beginning of water runoff. The I_a accounts for the depression storage due to surface roughness, canopy and litter interception, and pre-ponding soil infiltration. A study in a non-infiltrating and highly compacted lawn found an I_a (interception + depression storage) value of 6.8 mm, a value close to the observed value of 4.4 mm in our study (Muller and Thompson, 2009). Hence, measuring the amount of canopy interception may also be a key component to improve runoff prediction. To some extent, the meaning of I_{tf} in the interception process can considered analogous to the meaning og I_a in the runoff process.

To illustrate the potential impact of precipitation interception by turfgrass canopies like zoysiagrass and bentgrass over a larger spatial extent, we also quantified the median daily precipitation amount and the potential canopy interception amount for the contiguous United States. For this analysis, we used a multi-sensor gridded precipitation product from the US National Weather Service at 4-km spatial resolution for the period of 1 January 2017 to 31 December 2020 (Figure 1.5). Interestingly, 72% of the area of the contiguous US has a median

daily precipitation below the minimum interception storage capacity of 4.4 mm found in this study for zoysiagrass and bentgrass (Figure 1.5A). Considering the average interception losses during precipitation events >4.4 mm based on Equation 3, our analysis revealed that 45% of the area of the contiguous US could result in >50% of the annual precipitation being intercepted by canopies of zoysiagrass and bentgrass (Figure 1.5B). This exercise assumed that the findings in this study can be extrapolated to other regions. While these assumptions may not be valid over the entire territory and across seasons beyond those included in this study, this exercise allowed us to approximate the potential impact of turfgrass canopy interception on the national water balance.

Conclusions

Our study consisted of quantifying throughfall and canopy interception of zoysiagrass and creeping bentgrass during rainfall events using a new method based on co-located pluviometers with and without a turfgrass patches. This new method enables simultaneous measurements of throughfall and canopy interception of turfgrass at high temporal resolution under natural rainfall conditions. The method of the co-located pluviometers allowed us to clearly identify well-defined stages of the interception process that may also apply to other land covers beyond turfgrass consisting of (1) complete precipitation interception by the canopy, (2) characterized by both throughfall and canopy interception, (3) and drying of the canopy after the precipitation has ceased.

Interception losses during the study period ranged from 34% in zoysiagrass to 47% in bentgrass. On average, the point of throughfall was 4.4 mm, suggesting that precipitation events <4.4 mm are unlikely to reach the soil surface in healthy turfgrass mowed at typical golf course fairway heights. Throughfall occurred when the turfgrass patches reached between 44 and 50% of their

13

maximum water storage capacity. We encourage scientists and water managers to account for interception in water balance computations and irrigation scheduling routines. To our knowledge, this is the first study that provides detailed insights to understanding the interception dynamics in turfgrass and highlights the inefficient nature of small precipitation and irrigation events in turfgrass systems.

References

Beard JB, Turfgrass root basics. TURFAX. 2001;*9*(3), 4-5.

Beard JB, Turf management for golf courses. 2nd ed. Ann Arbor Press, Chelsea, MI. 2002.

Bremer DJ, Auen LM, Ham JM, Owensby CE, Evapotranspiration in a prairie ecosystem. Agronomy Journal. 2001;93(2):338–48.

Bremer DJ, Ham JM, Effect of spring burning on the Surface Energy Balance in a tallgrass prairie. Agricultural and Forest Meteorology. 1999;97(1):43–54.

Burgy RH, Pomeroy CR, Interception losses in grassy vegetation. Transactions, American Geophysical Union. 1958;39(6):1095.

Carlyle-Moses DE, Throughfall, stemflow, and canopy interception loss fluxes in a semi-arid Sierra Madre Oriental Matorral Community. Journal of Arid Environments. 2004;58(2):181–202.

Dunkerley D, Intra-event intermittency of rainfall: An analysis of the metrics of rain and no-rain periods. Hydrological Processes. 2015;29(15):3294–305.

Dunkerley D, Measuring interception loss and canopy storage in dryland vegetation: A brief review and evaluation of available research strategies. Hydrological Processes. 2000;14(4):669–78.

Dunkerley D, Sub-daily rainfall events in an arid environment with marked climate variability: Variation among wet and dry years at Fowlers Gap, New South Wales, Australia. Journal of Arid Environments. 2013;96:23–30.

Dunkerley D, Intra-storm evaporation as a component of canopy interception loss in dryland shrubs: Observations from Fowlers Gap, Australia. Hydrological Processes. 2008;22(12):1985–95.

Gash JH, An analytical model of rainfall interception by forests. Quarterly Journal of the Royal Meteorological Society. 1979;105(443):43–55.

Gerrits AM, Savenije HH, Hoffmann L, Pfister L, New technique to measure forest floor interception – an application in a Beech Forest in Luxembourg. Hydrology and Earth System Sciences. 2007;11(2):695–701.

Gilliam FS, Seastedt TR, Knapp AK, Canopy rainfall interception and throughfall in burned and unburned tallgrass prairie. The Southwestern Naturalist. 1987;32(2):267.

He Z-B, Yang J-J, Du J, Zhao W-Z, Liu H, Chang X-X, Spatial variability of canopy interception in a spruce forest of the semiarid mountain regions of China. Agricultural and Forest Meteorology. 2014;188:58–63.

Morris KE. National turfgrass research initiative. National Turfgrass Federation, Inc., and National Turfgrass Evaluation Program, Beltsville. 2003.

Mueller GD, Thompson AM, The ability of urban residential lawns to disconnect impervious area from municipal sewer systems. JAWRA Journal of the American Water Resources Association. 2009;45(5):1116–26.

Ochsner TE, Rain or shine: An introduction to soil physical properties and processes. 2022; p. 94-99. Published by Oklahoma State University Libraries under the Creative Commons Attribution 4.0 International License. doi.org/10.17605/OSF.IO/Z4RBT.

Parker N, Patrignani A, Reconstructing precipitation events using collocated soil moisture information. Journal of Hydrometeorology. 2021;22(12):3275–90.

Patrignani A, Knapp M, Redmond C, Santos E, Technical overview of the Kansas mesonet. Journal of Atmospheric and Oceanic Technology. 2020;37(12):2167–83.

Peel MC, Finlayson BL, McMahon TA, Updated world map of the Köppen-Geiger climate classification. Hydrology and Earth System Sciences. 2007;11(5):1633–44.

Peel MC, Finlayson BL, McMahon TA, Updated world map of the Köppen-Geiger climate classification. Hydrology and Earth System Sciences. 2007;11(5):1633–44.

Reid LM, Lewis J, Rates, timing, and mechanisms of rainfall interception loss in a coastal redwood forest. Journal of Hydrology. 2009;375(3-4):459–70.

Savenije, H.H., 2004. The importance of interception and why we should delete the term evapotranspiration from our vocabulary. Hydrological processes, 18(8), pp.1507-1511. doi: 10.1002/hyp.5563

Shachnovich Y, Berliner PR, Bar P, Rainfall interception and spatial distribution of throughfall in a pine forest planted in an arid zone. Journal of Hydrology. 2008;349(1-2):168–77.

Sheng H, Cai T, Influence of rainfall on canopy interception in mixed broad-leaved—Korean pine forest in xiaoxing'an mountains, northeastern China. Forests. 2019;10(3):248.

Taylor DH, Blake GR, The effect of turfgrass thatch on water infiltration rates. Soil Science Society of America Journal. 1982;46(3):616–9.

Throssell CS, Lyman GT, Johnson ME, Stacey GA, Brown CD, Golf Course Environmental Profile Measures Water Use, source, cost, quality, management and conservation strategies. Applied Turfgrass Science. 2009;6(1):1–20.

Tsiko CT, Makurira H, Gerrits AMJ, Savenije HHG, Measuring forest floor and canopy interception in a savannah ecosystem. Physics and Chemistry of the Earth, Parts A/B/C. 2012;47-48:122–7.

Yimam YT, Ochsner TE, Kakani VG, Evapotranspiration partitioning and water use efficiency of switchgrass and biomass sorghum managed for biofuel. Agricultural Water Management. 2015;155:40–7.

Zimmerman TL. The effect of amendment, compaction, soil depth, and time on various physical properties of physically modified Hagerstown soil. The Pennsylvania State University; 1973.

Zou CB, Caterina GL, Will RE, Stebler E, Turton D, Canopy interception for a tallgrass prairie under juniper encroachment. PLOS ONE. 2015;10(11).
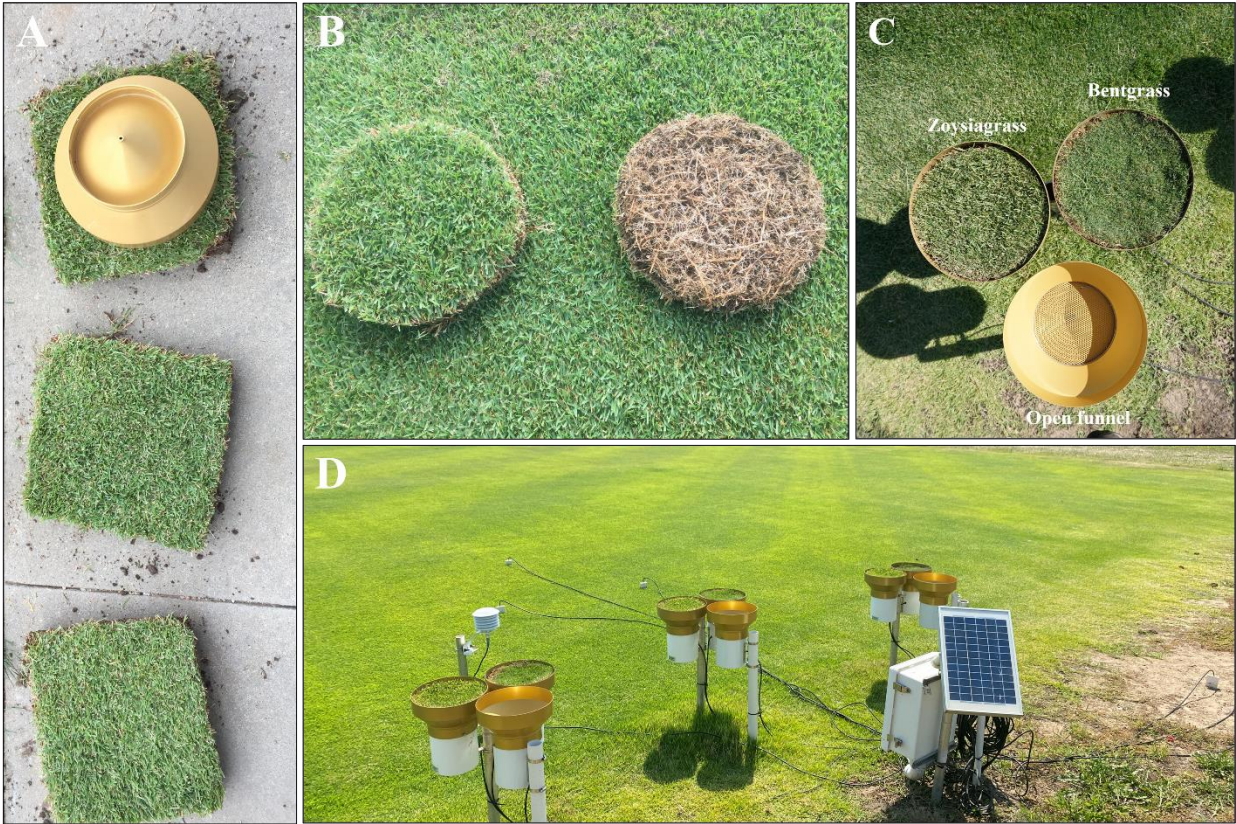
Figure 1.1 Figure illustrating A) the process of delineating and cutting the turfgrass patch using the pluviometer collector as template to ensure close fit, B) the top and bottom of a turfgrass patch after removing the soil attached to the bottom of the thatch layer and ready to be inserted into the pluviometer collector, C) a top view example of the pluviometers with and without the turfgrass patches of zoysiagrass and creeping bentgrass before the occurrence of a precipitation event, and D) the replicated field set up with showing three sets of three co-located pluviometers, a sensor for measuring air temperature and relative humidity, soil moisture sensors deployed in bare soil and below the surrounding zoysiagrass canopy, and associated logging hardware.
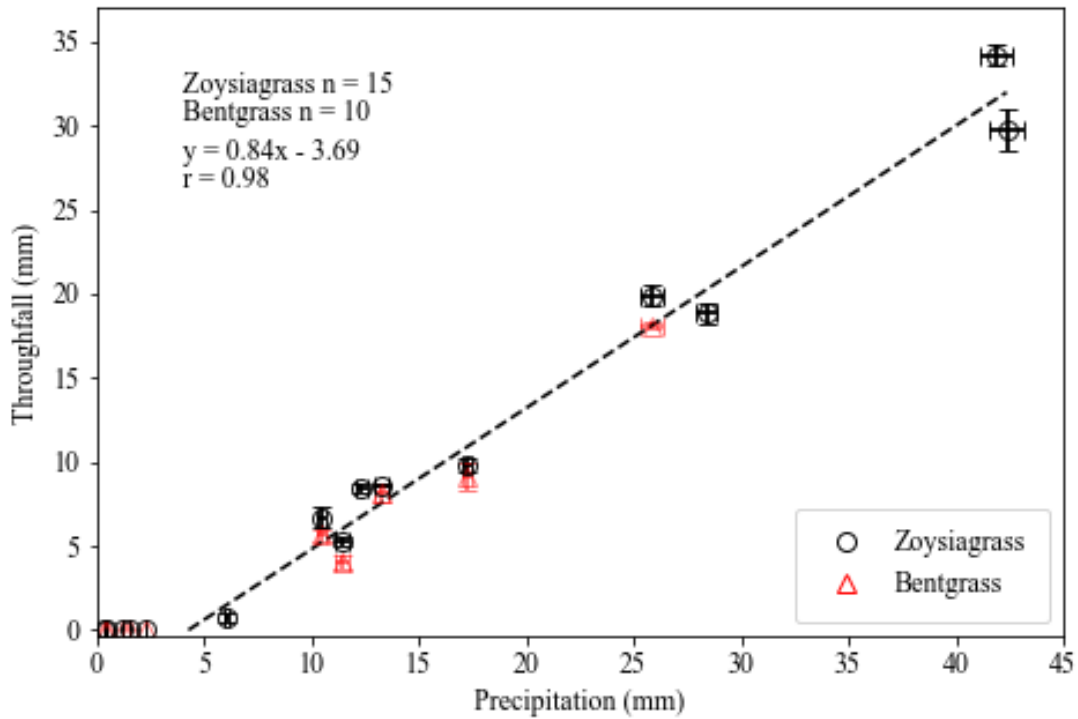
Figure 1.2 Relationship between precipitation and throughfall amount of patches of zoysiagrass and creeping bentgrass for all 15 natural storms. The *x*-intercept of 4.4 mm (95% CI [3.6, 5.3]) represents the minimum canopy interception before throughfall begins. The linear fitting exercise was done only using storm events that had throughfall >0 mm. Error bars represent the standard deviation of throughfall and precipitation. For some markers error bars are masked by the marker size.
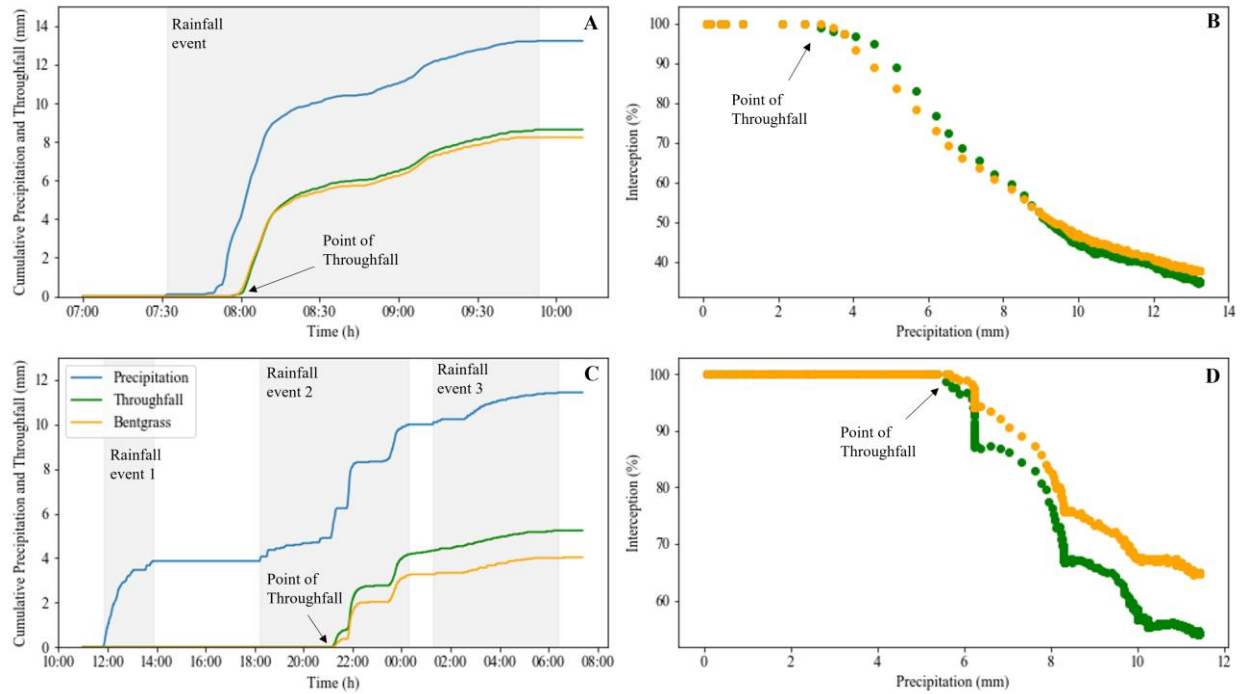
Figure 1.3 Comparison of cumulative precipitation, cumulative throughfall, and canopy interception for patches of zoysiagrass and creeping bentgrass during a storm with a single rainfall event (A and B, storm 14 in Table 1) and a storm with three rainfall events of variable lengths (C and D, storm 10 in Table 1). Both storms resulted in similar precipitation amount but had a different number of intra-storm precipitation events. The point of throughfall denoted by arrows.
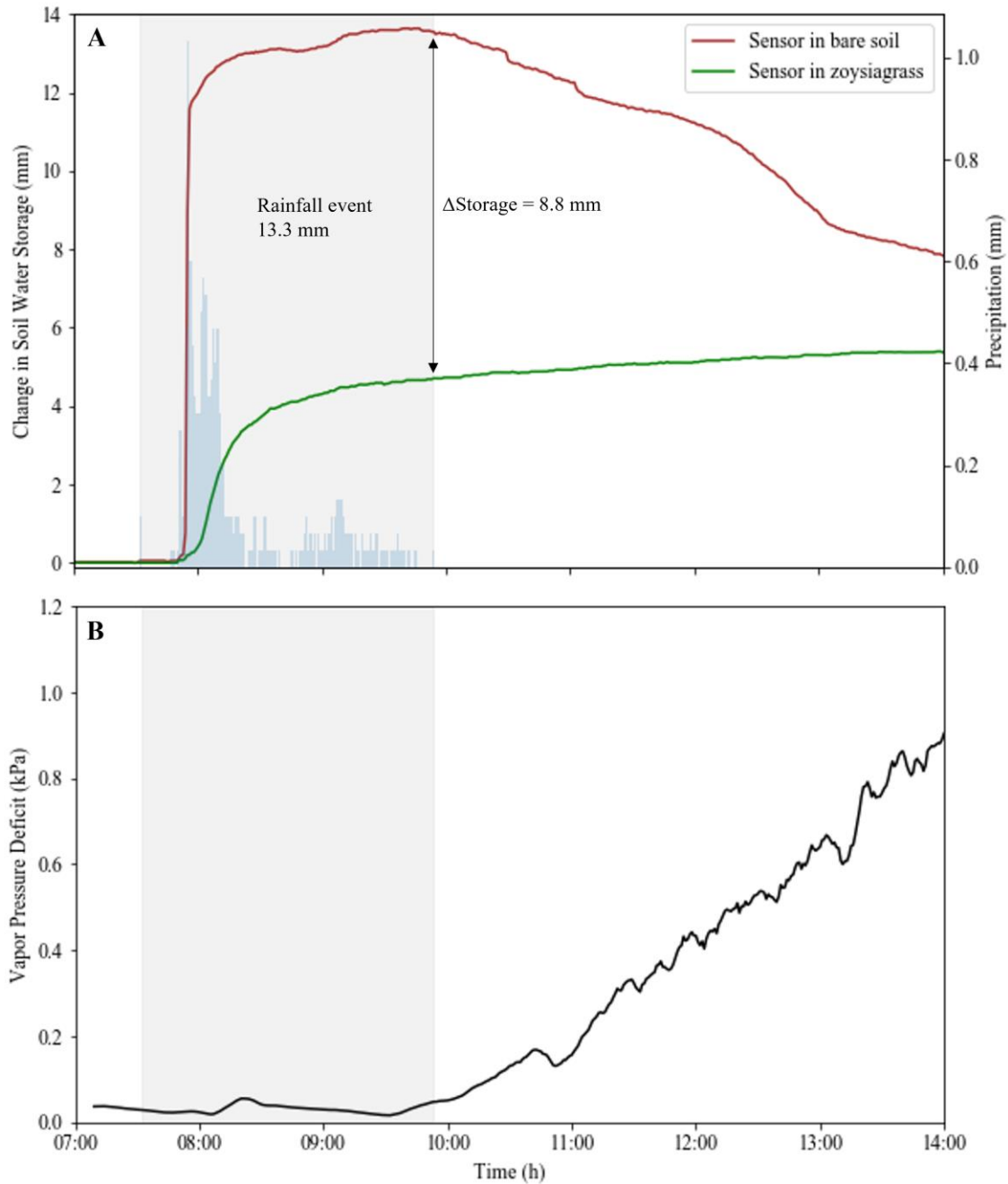
Figure 1.4 A) Changes in 1-minute soil water storage in the 0-12 cm soil layer measured with a vertically inserted soil water reflectometer in bare soil and in a Zoysiagrass canopy during a 13.3 mm rainfall event with a duration 2.5 hours on 22 May 2020 (Storm 14a); B) Vapor pressure deficit during and after the rainfall event. The post-storm decrease in soil water storage in Figure A is a result of soil moisture redistribution to deeper soil layer and evaporation driven by the increasing evaporative demand.
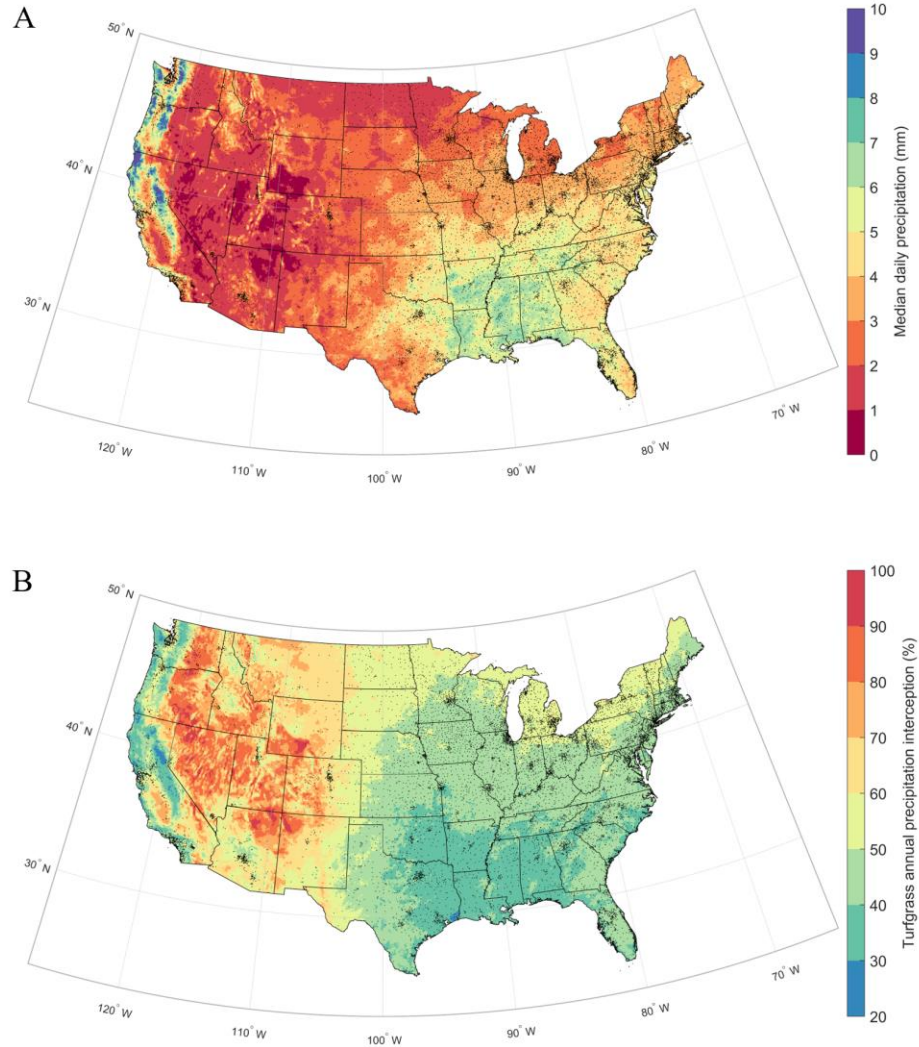
Figure 1.5 Maps showing the A) median daily precipitation totals for the contiguous United States in the period 2017-2020 from a multi-sensor gridded precipitation product at 4-km spatial resolution; and B) the estimated average percentage of annual precipitation intercepted by zoysiagrass and creeping bentgrass for the period 2017-2020 calculated using equations 2 and 3. Interception amount for daily precipitation events exceeding 45 mm was kept constant at a value of 11.4 mm [i.e., $I_{tf} + 0.16(45 - I_{tf})$, where $I_{tf} = 4.4$ mm] since our study did not include larger events. Only days with precipitation >0 mm were used to compute the maps. Black dots representing the locations of golf courses throughout the U.S.

Table 1.1 Table showing the duration, gross precipitation (P_g), precipitation maximum intensity (P_{imax}), throughfall (*TF*), interception until the point of throughfall (I_{tf}), and canopy interception (*I*) for each individual precipitation event across 15 storms for turfgrass patches of 'Meyer' zoysiagrass and creeping bentgrass. Canopy interception values in parenthesis represent the percentage of P_g. Values for each precipitation event are the average of three pluviometers.

				Zoysiagrass			Bentgrass		
Storm-Event	Duration	P_g	P_{imax}	TF	I_{tf}	I	TF	I_{tf}	I
	minutes	mm	mm hr^{-1}	mm	mm	mm	mm	mm	mm
1-a	86	40.3	97	32.9	6.4	7.4 (18)			
2-a	102	4.3	28	0.1	3.4	4.2 (98)			
2-b	66	1.7	22	0.7	1.1	1.1 (62)			
3-a	40	14.7	88	8.5	2.4	6.2 (42)			
3-b	211	3	18	0.8	1.7	2.2 (74)			
3-c	148	5.3	22	4.6	0.3	0.7 (14)			
3-d	74	5.4	60	5	0.3	0.4 (7)			
4-a	320	12	10	8.5	2.7	3.6 (30)			
4-b	37	0.3	4	0	—	0.3 (100)			
5-a	968	42.4	14	29.8	5.7	12.6 (30)			
6-a	178	2.3	6	0	—	2.3 (100)	0	—	2.3 (100)
7-a	390	8.7	12	5.3	3.3	3.4 (39)	4.5	3.4	4.2 (49)
7-b	347	1.7	4	1.4	0.3	0.3 (19)	1.1	0.5	0.6 (35)
8-a	38	0.5	4	0	—	0.5 (100)	0	—	0.5 (100)
9-a	24	0.3	2	0	—	0.3 (100)	0	—	0.3 (100)
9-b	265	1.3	10	0	—	1.3 (100)	0	—	1.3 (100)
10-a	120	3.9	8	0	—	3.9 (100)	0	—	3.9 (100)
10-b	363	6.1	18	4.3	1.9	1.8 (29)	3.3	2.2	2.9 (47)
10-c	305	1.4	6	0.9	0.1	0.5 (37)	0.8	0.2	0.7 (47)
11-a	32	1.2	6	0	—	1.2 (100)	0	—	1.2 (100)
11-b	27	0.1	2	0	—	0.1 (100)	0	—	0.1 (100)
12-a	23	0.4	4	0	—	0.4 (100)	0	—	0.4 (100)
13-a	241	25.8	72	19.9	5.4	5.9 (23)	18.1	7.1	7.7 (30)
14-a	141	13.2	62	8.6	3.5	4.6 (35)	8.2	4	5 (38)
15-a	360	17.3	44	9.8	5.3	7.4 (43)	9.1	4.3	8.2 (48)
Total	4906	213.6		141.1		72.6			39.3

24

Table 1.2 Storm, storage capacity, dry biomass, thatch layer for turfgrass patches of zoysiagrass and bentgrass. Value between parenthesis represent the standard error of the mean.

Storm	Storage Capacity	Dry Biomass	Patch Layer Thickness
	mm	g	mm
Zoysiagrass			
1	10.1 (0.3)	444 (12.3)	42 (0.5)
2	9.8 (0.4)	430 (9.1)	46 (0.4)
3	9.4 (0.4)	479 (18.9)	47 (0.4)
4	9.7 (0.2)	483 (3.2)	47 (0.5)
5	9.5 (0.6)	447 (20.8)	42 (0.4)
6	9.9 (0.4)	462 (22.5)	48 (0.3)
7	9.6 (0.7)	424 (8.5)	48 (0.7)
8	8.0 (0.5)	356 (51.6)	43 (0.2)
9	8.2 (0.7)	391(67.2)	46 (0.5)
10	9.6 (0.3)	402 (45.6)	46 (0.4)
11	6.1 (0.4)	325 (24.8)	45 (0.3)
12	7.7 (0.6)	485 (26.9)	47 (0.3)
13	7.1 (0.3)	332 (44.9)	46 (0.3)
14	11.1 (0.3)	361 (4.5)	45 (0.3)
15	9.4 (0.3)	578 (25.7)	47(0.2)
Bentgrass			
6	8.7 (0.9)	314 (13)	28 (0.4)
7	8.6 (0.2)	196 (35)	24 (0.4)
8	7.5 (0.4)	204 (23)	24 (0.7)
9	8.8 (2.6)	161 (19)	23 (0.5)
10	10.0 (0.7)	150 (19)	24 (0.4)
11	8.9 (0.5)	164 (29)	24 (0.4)
12	11.4 (1.4)	249 (56)	23 (0.4)
13	7.0 (2.8)	293 (75)	24(0.4)
14	10.9 (0.3)	337 (39)	26 (0.3)
15	9.4 (0.7)	316 (44)	24 (0.4)

Chapter 2 - Irrigation Decision Tree for Water Management in Turfgrass Systems

Abstract

Irrigation strategies used by homeowners, golf courses, and athletic fields often rely on calendar schedules or deficit irrigation strategies that ignore soil moisture. The turfgrass industry has not taken full advantage of soil moisture sensor (SMS) technology because of cost and a lack of research into fundamental questions such as sensor placement, soil moisture thresholds for initiating irrigation, and unknown quantitative relationships between soil moisture and turfgrass quality. To address some of these questions we developed an "irrigation decision tree" (DT) that incorporates SMS, turfgrass canopy condition, and forecasted precipitation, all components of the soil-plant-atmosphere continuum, to improve the timing and amount of each irrigation event. The effects of DT-based irrigation, traditional-based irrigation, and evapotranspiration (60% ET) -based irrigation scheduling was investigated at Manhattan, KS on 'Meyer' zoysiagrass (*Zoysia japonica* L.), to compare the turf canopy response to soil moisture. During 2019, soil moisture thresholds ranging from 0.185 m^3m^{-3} to 0.225 m^3m^{-3} were determined based the onset of canopy stress to available water capacity and then integrated into the 2020 growing season. Additionally, we showed when incorporating multiple data-driven thresholds comprising of soil moisture, plant canopy conditions, and forecasted precipitation into a decision tree during the 2020 season, as opposed to a single variable (SMS) threshold in 2019, better irrigation timing and water savings were achieved. Water savings of 81% were achieved during 2020 compared to 66% during 2019. Incorporation of such a decision tree in irrigation practices by turfgrass managers may enable them to maintain good quality turfgrass with significantly less water.

Introduction

In the United States, there are an estimated 600,000 hectares of irrigated turfgrass in golf courses, which use approximately 2.2 km^3 of water per year (Throssell et al., EIFG, 2015). Current irrigation strategies used by golf courses and athletic fields often rely on calendar schedules or deficit irrigation strategies that completely ignore soil moisture conditions. Since turfgrass is a relatively shallow-rooted crop that relies on adequate soil water storage to cope with the atmospheric demand, integrating information from soil moisture sensors (SMS) to existing irrigation techniques has the potential to substantially improve the timing and amount of each irrigation event. Incorporating information from SMS to control irrigation has resulted in up to 70% water savings in lawn-or rough-height turfgrass, with greater savings in humid than dry climatic conditions (Chabon et al., 2017; Dukes, 2012). The incorporation of smart irrigation controllers that take advantage of weather data for estimating turfgrass evapotranspiration (ET) rates, precipitation, and soil moisture have shown to reduce the amount and frequency of irrigation without negatively affecting turfgrass quality (Serena et al., 2020). A study conducted in Wimauma, Florida on St. Augustinegrass (*Stenotaphrum secundatum*) found water savings of 43% during a 15-month period using ET-based irrigation compared to calendar-based frequency irrigation (Davis et al., 2009). Furthermore, in Citra, Florida, water savings of 7-30% were achieved when using rain sensors and 0-74% when using SMS for controlling irrigation compared to a time-based treatment in St. Augustinegrass, also (McCready et al., 2009). The integration of machine learning algorithms with real time weather observations to predict the optimal time of day to irrigate can result in up to 60% more water savings compared with traditional irrigation scheduling (Gloria et at., 2021).

In golf courses, fairways represent about 30% of the turfgrass area in a typical 18-hole golf course (EIFG, 2007). To our knowledge, the potential water savings of using SMS to control irrigation in golf course fairways has not been reported in the scientific literature. Sensors Magazine reported the Desert Mountain Golf Course, in Arizona, had 15-20% water savings by using SMS to control irrigation on their fairways and greens (Kevan, 2006). Golf courses have not taken full advantage of soil moisture technology in fairways, possibly because of cost, but also because of a lack of research on fundamental questions such as sensor placement, soil moisture thresholds for initiating irrigation, and unknown quantitative relationships between soil moisture and turfgrass quality.

We hypothesize that combining real-time soil moisture information, turfgrass canopy conditions, and precipitation forecasts will improve irrigation scheduling and reduce total water use relative to calendar schedules. The objectives of this study were to: (1) determine turf canopy responses to plant available water and (2) compare a decision tree-based irrigation method that integrates soil moisture information, turf canopy conditions, and precipitation forecasts against traditional-based irrigation and 60% ET-based irrigation scheduling.

Materials and Methods

Experiment Layout

The study was conducted at the Rocky Ford Turfgrass Research Center near Manhattan, Kansas (39°13'59.628" N, 96°34'30.612" W) from 1 June through 30 September during the 2019 and 2020 growing seasons. The experimental site belongs to the Dfa Köppen-Geiger climate classification, which is characterized by humid continental hot summers with year-round precipitation (Peel, 2007). The average annual temperature at the site is 13.4 °C and the average annual precipitation is 895 mm (NOAA Climate.gov). This research was conducted on 'Meyer'

zoysiagrass (*Zoysia japonica* L.) using a Latin square design with four irrigation treatments and four replications (total of 16 plots). The treatments consisted of a (1) traditional frequency-based irrigation (traditional), receiving 12.7 mm of water two times per week regardless of the weather conditions, (2) deficit irrigation based on replacement of 60% grass reference ET (ET_o), split into two applications per week, (3) irrigation based on the decision tree (DT) incorporating soil moisture, canopy cover conditions, and probability of precipitation for the next day, and (4) a check treatment with zero irrigation (i.e., rainfed treatment). The probability of precipitation is defined as the probability that a given location will receive at least 0.254 mm of precipitation (https://www.weather.gov/ffc/pop). In 2019, we only utilized soil moisture information to trigger irrigation in the SMS plots and used results from that year to investigate the plant canopy response to soil water deficits, given the silt loam properties of the soil as determined in the laboratory. The DT was then used in 2020 using soil moisture thresholds developed in 2019.

Each plot was equipped with traditional overhead sprinklers (model T5 series rotors, Toro Company) and had dimensions of 8 by 8 m. Irrigation amounts were determined by conducting a catch-can irrigation audit of the sprinklers prior to initiation of the study in both years. The turfgrass height of cut was 16 mm, imitating the maintenance of a golf course fairway. Plots were fertilized the first week of June and last week in July at 24.4 kg N ha^{-1} using an 18-24-12 formulation (The Andersons, Inc.). No cultural practices (i.e., aeration or vertical mowing) were conducted throughout the study due to buried soil moisture sensors and associated cables.

Characterizing Soil Physical Properties

Undisturbed soil cores were collected a depth of 7.5 cm to 12.5 cm using stainless-steel rings with a volume of 250 cm^3 from each of the 16 plots to characterize the soil physical

properties. Effective saturation was measured by placing the samples in a solution of 5 mM

$CaCl_2$ for 24 hours. Soil water retention in the range from 0 to -80 kPa was measured using

precision mini-tensiometers (model HYPROP, Meter Group, Inc.). Soil water retention below -

500 kPa was measured by extracting small subsamples along the wetting front using a dew point

soil water potential meter (model WP4C, Meter Group, Inc.). By combining data from both

instruments, a full range moisture release curve was generated for each plot. Effective saturation

of the soil averaged 39.5% and the bulk density averaged 1.51 g cm^{-3}. The fraction of sand, silt,

and clay for each plot was determined using the hydrometer method (Gavlak, 2005). Silt loam

was the determined soil texture classification with an average of 12% $\pm$ 3% sand and 38% $\pm$ 2%

clay.

Decision tree

In 2020 we advanced the SMS irrigation method by incorporating a decision tree DT to

determine when to irrigate (Figure 2.1). The decision tree helped determine a course of action by

providing a series of questions that centered around each of the soil-plant-atmosphere

components. The first criterion for triggering irrigation with the DT-based treatment was when

volumetric water content (VWC) reached a critical threshold range between 22.5% and 18.5%.

However, irrigation was delayed unless a second criterion was reached, which was when green

canopy cover (GCC) in the DT treatment declined to >5% less in the traditional irrigation

treatment. This threshold was used because, from a turfgrass quality perspective, the traditional

irrigation approach experienced minimum drought stress and naturally retained high turfgrass

quality throughout the growing season. Finally, irrigation was delayed even further if the

forecasted probability of precipitation within the next 24 hours was >50%, at the time when the

first two criteria had been reached. Thus, the best-informed decision for irrigation was

determined by processing data from field measurements and weather data along with these questions in the decision tree.

Instrumentation

Soil moisture sensors (CS655, Campbell Sci. Logan, UT) were installed horizontally at 10 cm depth in the center of each plot. Soil moisture was measured every 15 minutes and averaged and recorded hourly using a datalogger (model CR1000, Campbell Scientific, Inc.). Soil moisture sensors were calibrated using packed soil columns of known volumetric water content in laboratory conditions. The known volumetric water content of each container determined using the thermos-gravimetric method and the apparent dielectric permittivity obtained from the sensor were used to develop a correction equation (Patrignani et al., 2022). Green canopy cover was measured directly over the buried sensors three to five times weekly with digital images (Nikon D5000, Nikon Inc.) using a lighted camera box. Images were analyzed with the Matlab version of the Canopeo application (Patrignani and Ochsner, 2015). Measurements of normalized difference vegetation index (NDVI) were also taken directly over the buried sensors as an auxiliary variable with a handheld device (RapidScan CS-45, Holland Scientific Inc.) Weather data were collected from an on-site Kansas Mesonet weather station (Patrignani et al. 2020) to track air temperature, relative humidity, and precipitation throughout the growing season. Precipitation forecast conditions were obtained from the local national weather service. All data analysis was performed using the Python programming language (Python Software Foundation, version 3.1. available at http://www.python.org).

Results and Discussion

Plant Available Water Capacity

Plant available water capacity (AWC) is defined as the amount of water a specific soil type can store that is available for plant use. It can be estimated by computing the differences between soil water content (θ) at field capacity (θ_{fc}) and soil water content at permanent wilting point (θ_{wp}) (Ochsner, 2019). To normalize AWC, the fraction of available water (FAW) capacity can be computed by:

$$FAW = (\theta - \theta wp / (\theta fc - \theta wp) \qquad \text{Eq. [1]}$$

We determined AWC in the laboratory by utilizing site-specific soil properties to characterize soil texture and model the relationship between matric water potential and VWC. A soil water retention curve was generated using the van Genuchten model (van Genuchten, 1980) (Figure 2.2). Upper and lower limits were considered using the least limiting water range, which defines the region bounded by upper and lower soil water content in which water, oxygen, and mechanical resistance become major limiting factors for root growth (da Silva et al., 1994). Critical values for crop growth are associated with the soil moisture at field capacity (-10 or -33 kPa) or at air-filled porosity of 10% for the upper limit (whichever is smaller), and the water content of permanent wilting point (-1500 kPa) for the lower limit (Safadoust et al., 2004). We used the least limiting range to define the upper and lower limits, which were set at 10% air-filled porosity (upper limit) and -1500 kPa (lower limit) (Figure 2.2). The soil water storage in the top X cm was calculated as:

$$S = \theta \times \Delta z \qquad \text{Eq. [2]}$$

Where S is soil water storage (mm), θ is the average volumetric water content of the soil layer (cm^3 cm^{-3}), and Δz is thickness of the soil layer (mm). By measuring the VWC within the soil

layer, we could then calculate the amount of water desired to refill the rootzone profile back to the upper limit. In this study we used a soil thickness of 20 cm, which represents the portion of the soil profile with substantial roots. This decision was verified by collecting two soil cores per plot with a diameter of 5 cm and visually inspecting the rooting depth in the top 50 cm of the soil profile. To determine the irrigation amount, we also estimated that an additional 5 mm of irrigation should be applied to account for interception by the canopy when watering the DT treatment (Chapter 1). Canopy interception was not considered in the traditional and the 60% ET treatments.

2019 Season

Total precipitation was 601 mm between the June-1 and August-31 in 2019, which was 233 mm above average the 30-year average for those months (Table 1.1). This large amount of precipitation minimized drought stress throughout the growing season. However, a dry period at the end of July resulted in a slight soil water deficit. This was the only period in 2019 when irrigation was triggered, which was based solely on SMS data, depicted by the blue arrows (Figure 2.3C); recall this was before development of the decision tree treatment that was implemented in 2020. Irrigation was intentionally triggered slightly later for the second irrigation event (second arrow) to determine when stress became evident in the canopy of SMS-based plots. Furthermore, the check treatment provided valuable information by allowing us to continue to monitor the canopy stress as VWC continued to decline (Figure 2.3C). During this period in late July, GCC decreased by 11%, from 98% to 87%, and then recovered after a rainfall event of 3.1 mm (Figure 2.3B). A drop in green biomass was also detected by the NDVI sensor, which followed a similar trend by decreasing 0.77 to 0.65 and then rebounding (Figure 2.3A). There was a strong correlation between GCC and NDVI with a R^2 value of 0.80, during this

decline and recovery period; the close relationship between GCC and NDVI in turfgrass has also been reported by others (Bell et al., 2002; Bremer et al., 2011).

A value of 0.5 FAW in the soil is often used as an approximate threshold for vegetative moisture stress (Allen et al., 1998). However, in the check treatment during this soil water deficit period, the turfgrass canopy experienced the onset of stress between 0.60 to 0.75 FAW, which relates to 18.5 to 22.5% VWC (Figure 2.4). These evaluations of the response of the plant canopy to soil moisture decline allowed us to develop accurate thresholds for determining irrigation timing for the following 2020 season. The total water applied to each irrigation treatment during the 2019 season was 156 mm in traditional treatment, 119 mm in the 60% ET treatment, and 53 mm in SMS treatment. The SMS-based irrigation approach applied 66% less water than the traditional treatment and 56% less water than the 60% ET treatment.

2020 Season

In the 2020 growing season we adopted the decision tree that integrated soil moisture information, canopy cover conditions, and the forecasted chance of precipitation to guide irrigation decisions (Figure 1.1). Total precipitation during the 2020 field study (i.e., 1 June to 31 August) was 289 mm, with highest rainfall events occurring in July (Figure 2.5, Table 1.1). The longest consecutive period without rainfall was 11 days in late August. Supplemental irrigation for each irrigation treatment during 2020 was 268 mm in traditional, 153 mm in deficit 60% ET, and 51 mm in DT-based plots. Thus, irrigation with the DT-based irrigation approach saved 81% of water compared with traditional irrigation scheduling and 67% of water compared with the 60% ET-based irrigation scheduling. Interestingly, water savings were greater in 2020 than 2019, despite 52% less precipitation in 2020 than in 2019. This outcome is counterintuitive but can be attributed to the incorporation of the DT method as described below.

To illustrate how the decision tree guided our irrigation management decisions, Figure 2.6 depicts when irrigation was applied during 2020. Pronounced soil drying occurred only during two periods in 2020, including at the end of June and again in late August (Figure 2.6B). During these periods, VWC in the DT-based reached the VWC threshold for triggering irrigation in the DT-based treatment, noted by the four arrows (Figure 2.6B). However, the two blue arrows were the only periods where all thresholds for triggering irrigation in the decision tree were met during the 2020 growing season. During these two periods, soil moisture in DT-based reached the VWC threshold range, GCC had dropped below 5% of the traditional treatment, and a chance of rainfall was < 50%. However, the two black arrows denote when VWC for the DT-based treatment reached the VWC threshold range, but GCC had not dropped below 5% of the traditional treatment, indicating canopy stress was not yet observed. Also, precipitation events shortly followed which allowed us to bypass the necessity for irrigating the DT-based treatment. This demonstrates how delaying irrigation as feasible can improve the chance that rainfall will occur, which further delays the need for irrigation (Cardenas-Lailhacar et al., 2008, 2010; Chabon et al., 2017).

When assessing the first drought period, in June, irrigation was triggered when VWC had declined to the irrigation threshold ($0.215m^3m^{-3}$), GCC in the DT-based treatment (82.7%) was >5% lower than in the traditional treatment (88.6%) (Figure 2.6A and 2.6B). Additionally, forecasted precipitation was <50%. Thereafter, in the check treatment, VWC continued to decrease to $0.19 m^3m^{-3}$ and GCC declined to 78%, before a precipitation event (Figure 2.6A and 2.7A). The effects of drought in unirrigated turfgrass were even more pronounced in August when GCC in the check treatment had decreased to 72.8% only three days after irrigation was triggered in the DT-based treatment (Figure 2.7B). During this period, VWC had reached the

irrigation threshold ($0.22m^3m^{-3}$), GCC had dropped to 92.1%, which was >5% lower than the

traditional irrigation plots, and forecasted precipitation was <50% (Figure 2.6). The FAW had

also declined to 0.59 in the check treatment (Figure 2.6B). This further illustrates how using this

method saves water, but that timing of irrigation is critical.

The soil water content for both the traditional and 60% ET treatments never dropped

below the upper limit of AWC throughout the entire season of 2020 (Figure 2.6B), which

indicates that irrigation was over applied with these methods. ET-based irrigation scheduling

only accounts for atmospheric conditions without allowing for soil moisture present in the

rooting profile.

Among treatments in 2020, GCC fell more than 5% below the traditional frequency-

based irrigation treatment for 20 days in the check treatment, 2 days in DT-based, and 0 days in

60% ET (Figure 2.8). Therefore, by applying only 51 mm of irrigation in the DT-based

treatment, we were able to avoid 18 days of less than desired canopy cover. This highlights how

turf quality in DT-based treatments was not compromised throughout the 2020 season while

achieving significant water savings.

Single variable thresholds (i.e., ET rates or soil moisture) have been applied in irrigation

management decisions but did not incorporate a decision tree (Domenghini et al., 2013; Chabon

et al., 2017; Braun and Bremer, 2019). The value of using a decision tree to save water in lieu of

only SMS data is illustrated by comparing irrigation in 2019, when only SMS data were used to

trigger irrigation, with 2020, when the irrigation decision tree was incorporated to trigger

irrigation. The amount of irrigation water applied in the SMS treatment in 2019 resulted in 53

mm and 51 mm in DT-based in 2020. However, in 2019 more than twice the amount of

precipitation was received compared to 2020 (Figure 2.9). We speculate that if we would have

incorporated our decision tree method during 2019, irrigation would have been only triggered once as opposed to twice, based on the rate of decline from the check treatment (Figure 2.3). By simply incorporating two more variables or questions to drive our irrigation decisions (i.e., green canopy cover and forecasted precipitation), even greater water savings were attained. Utilizing a data-driven decision tree as a guide by using various sensor technologies yielded significant water savings.

Conclusions

Turfgrass irrigation based on a simple decision-tree that integrated the components of the soil-plant-atmosphere continuum used 81% less water compared to traditional calendar-based irrigation in 2020. Incorporating rootzone soil moisture information, canopy cover conditions, and 24-hour probability of forecasted precipitation allowed us to gain considerable insight into the response of the turf canopy as FAW declined with drying soils during droughty periods. Soil moisture thresholds were determined during the 2019 growing season and then integrated into the DT treatment in 2020. Furthermore, we showed that by incorporating VWC, GCC, and forecasted precipitation into a decision tree during 2020, as opposed to a single variable threshold of soil moisture in 2019, better timing of irrigation and a 14% increase in water savings were achieved. This integrating of data from each component of the soil-plant-atmosphere continuum proved to be a successful method to drive our irrigation management decisions. Traditional-based and ET-based irrigation methods significantly over applied and unnecessarily wasted water without providing significantly greater benefit or quality to the turfgrass canopy.

The information gained from this research may provide turfgrass managers with a more practical way of interpreting soil moisture, plant canopy conditions, and weather data to enable them to make meaningful changes in their irrigation practices. Future research should explore

other current and emerging sensing technologies that could be integrated into this or similar

decision trees to improve data-driven irrigation management decisions.

References

Allen, R.G., Pereira, L.S., Raes, D., and. Smith, M. (1998). Crop evapotranspiration: Guidelines for computing crop water requirements. FAO Irrigation and Drainage Paper No. 56., FAO, Rome, Italy.

Bell, G. E.,Martin, D. L.,Wiese, S. G., Dobson, D. D., Smith, M. W., Stone, M. L., & Solie, J. B. (2002). Vehicle-mounted optical sensing: An objective means for evaluating turf quality. Crop Science, 42, 197–201. https://doi.org/10.2135/cropsci2002.1970

Braun, R. C., & Bremer, D. J. (2019). Carbon sequestration in zoysiagrass turf under different irrigation and fertilization management regimes. *Agrosystems, Geosciences & Environment, 2*(1), 1-8. doi:10.2134/age2018.12.0060

Bremer, D. J., Lee, H., Su, K., & Keeley, S. J. (2011). Relationships between normalized difference vegetation index and visual quality in cool-season turfgrass: II. Factors affecting NDVI and its component reflectances. Crop Science, 51, 2219–2227. https://doi.org/10.2135/cropsci2010.12.0729

Cardena-Lailhacar, B., Dukes, M. D., & Miller, G. L. (2008). Sensor-based automation of irrigation on Bermudagrass, during wet weather conditions. *Journal of Irrigation and Drainage Engineering, 134*(2), 120-128. doi:10.1061/(asce)0733-9437(2008)134:2(120)

Cardenas-Lailhacar, B., Dukes, M. D., & Miller, G. L. (2010). Sensor-based automation of irrigation on Bermudagrass during dry weather conditions. *Journal of Irrigation and Drainage Engineering, 136*(3), 184-193. doi:10.1061/(asce)ir.1943-4774.0000153

Chabon, J., D.J. Bremer, J.D. Fry, and C. Lavis. (2017). Effects of soil moisture-based irrigation controllers, mowing height, and trinexapac-ethyl on tall fescue irrigation amounts and mowing requirements. Int. Turf. Soc. Res. J.13:1-6. doi:10.2134/itsrj2016.04.0242

da Silva, A. P., Kay, B. D., & Perfect, E. (1994). Characterization of the least limiting water range of soils. *Soil Science Society of America Journal, 58*(6), 1775. doi:10.2136/sssaj1994.03615995005800060028x

Davis, S., Dukes, M., & Miller, G. (2009). Landscape irrigation by evapotranspiration-based irrigation controllers under dry conditions in southwest Florida. *Agricultural Water Management, 96*(12), 1828-1836. doi:10.1016/j.agwat.2009.08.005

Domenghini, J. C., Bremer, D. J., Fry, J. D., & Davis, G. L. (2013). Prolonged drought and recovery responses of Kentucky bluegrass and ornamental groundcovers. *HortScience, 48*(9), 1209-1215. doi:10.21273/hortsci.48.9.1209

Dukes, M. D. (2012). Water conservation potential of landscape irrigation smart controllers. *Transactions of the ASABE, 55*(2), 563-569. doi:10.13031/2013.41391

EIFG (Environmental Institute for Golf), 2007. Golf course environmental profile: Property profile and environmental stewardship of golf courses. Volume 1 Summary

EIFG (Environmental Institute for Golf), 2015. Golf course environmental profile: Water use and conservation practices in golf courses. Phase 2. Volume 1:1-31

Gavlak, R., Horneck, D., and Miller, R. (2005). Plant, soil and water reference methods for the Western Region. Western Regional Extension Publication (WREP) 125, WERA-103 Technical Committee. http://www.naptprogram.org/files/napt/western-states-method-manual-2005.pdf.

Glória, A., Cardoso, J., & Sebastião, P. (2021). Sustainable irrigation system for farming supported by machine learning and real-time Sensor Data. *Sensors, 21*(9), 3079. doi:10.3390/s21093079

Kevan, T., (2006). Irrigation smarts tee up savings: Wireless technology moves sensors to the

    greens and fairways of leading golf courses, and enables cost savings. Sensors Magazine

    23.11 (Nov.) p. S4.

McCready, M., Dukes, M., & Miller, G. (2009). Water conservation potential of smart irrigation

    controllers on St. Augustinegrass. *Agricultural Water Management, 96*(11), 1623-1632.

    doi:10.1016/j.agwat.2009.06.007

Ochsner, T. (2019). Rain or shine: An introduction to soil physical properties and processes. 242-

    243. doi:10.22488/okstate.21.000000

Patrignani, A., Knapp, M., Redmond, C. and Santos, E. (2020). Technical overview of the

    Kansas Mesonet. *Journal of Atmospheric and Oceanic Technology*, *37*(12), pp.2167-

    2183.

Patrignani, A., Ochsner, T. E., Feng, L., Dyer, D., & Rossini, P. R. (2022). Calibration and

    validation of soil water reflectometers. *Vadose Zone Journal*, e20190.

Patrignani, A., & Ochsner, T. E. (2015). Canopeo: A powerful new tool for measuring fractional

    green canopy cover. *Agronomy Journal, 107*(6), 2312-2320. doi:10.2134/agronj15.0150

Peel, M. C., Finlayson, B. L., & McMahon, T. A. (2007). Updated world map of the Köppen-

    Geiger climate classification. *Hydrology and Earth System Sciences, 11*(5), 1633-1644.

    doi:10.5194/hess-11-1633-2007

Safadoust, A., Feizee, P., Mahboubi, A., Gharabaghi, B., Mosaddeghi, M., & Ahrens, B. (2014).

    Least limiting water range as affected by soil texture and cropping system. *Agricultural*

    Water Management, 136, 34-41. doi:10.1016/j.agwat.2014.01.007

Serena, M., Velasco-Cruz, C., Friell, J., Schiavon, M., Sevostianova, E., Beck, L., Sallenave, R., Leinauer, B. (2020). Irrigation scheduling technologies reduce water use and maintain turfgrass quality. *Agronomy Journal, 112*(5), 3456-3469. doi:10.1002/agj2.20246

Throssell, C. S., Lyman, G. T., Johnson, M. E., Stacey, G. A., & Brown, C. D. (2009). Golf Course Environmental Profile Measures Water Use, source, cost, quality, management and conservation strategies. *Applied Turfgrass Science, 6*(1), 1-20. doi:10.1094/ats-2009-0129-01-rs

Van Genuchten, M. T. (1980). A closed-form equation for predicting the hydraulic conductivity of unsaturated soils. *Soil Science Society of America Journal, 44*(5), 892-898. doi:10.2136/sssaj1980.03615995004400050002
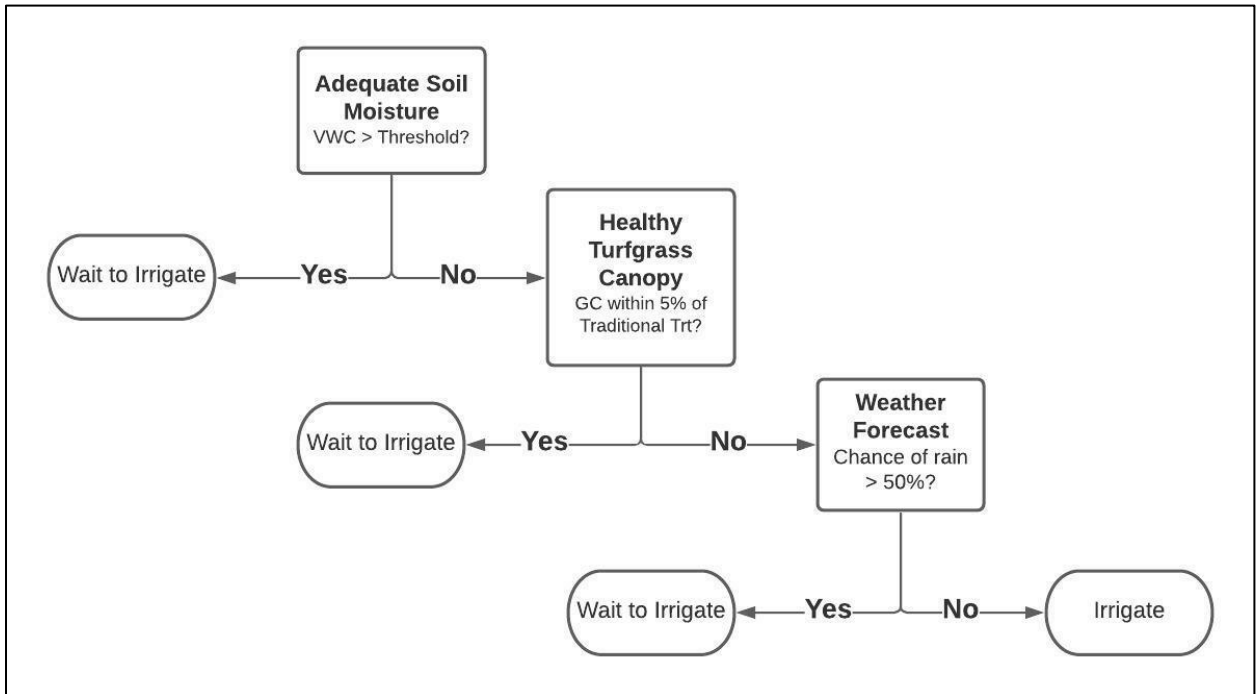
Figure 2.1 Decision tree based on components of the soil-plant-atmosphere continuum to guide irrigation scheduling.
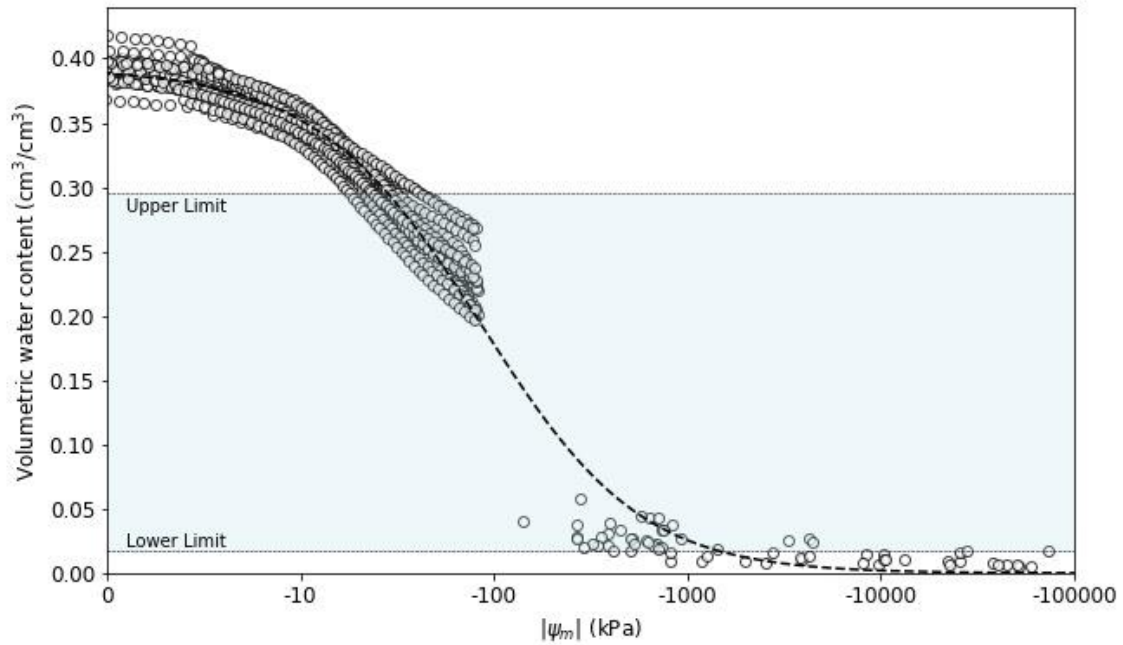
Figure 2.2 Soil water retention curve for a silt loam soil with a bulk density of 1.51 g cm^{-3}. Markers represent observations and the dashed line represents the van Genuchten model. The lower limit was estimated as the volumetric water content at -1500 kPa and the upper limit was estimated as the volumetric water content at which the soil has a 10% air-filled porosity. The plant available water capacity is indicated by the shaded area. Note that the typical definition of field capacity using a volumetric water content at -10 kPa would result in air-filled porosity <10% for this soil.
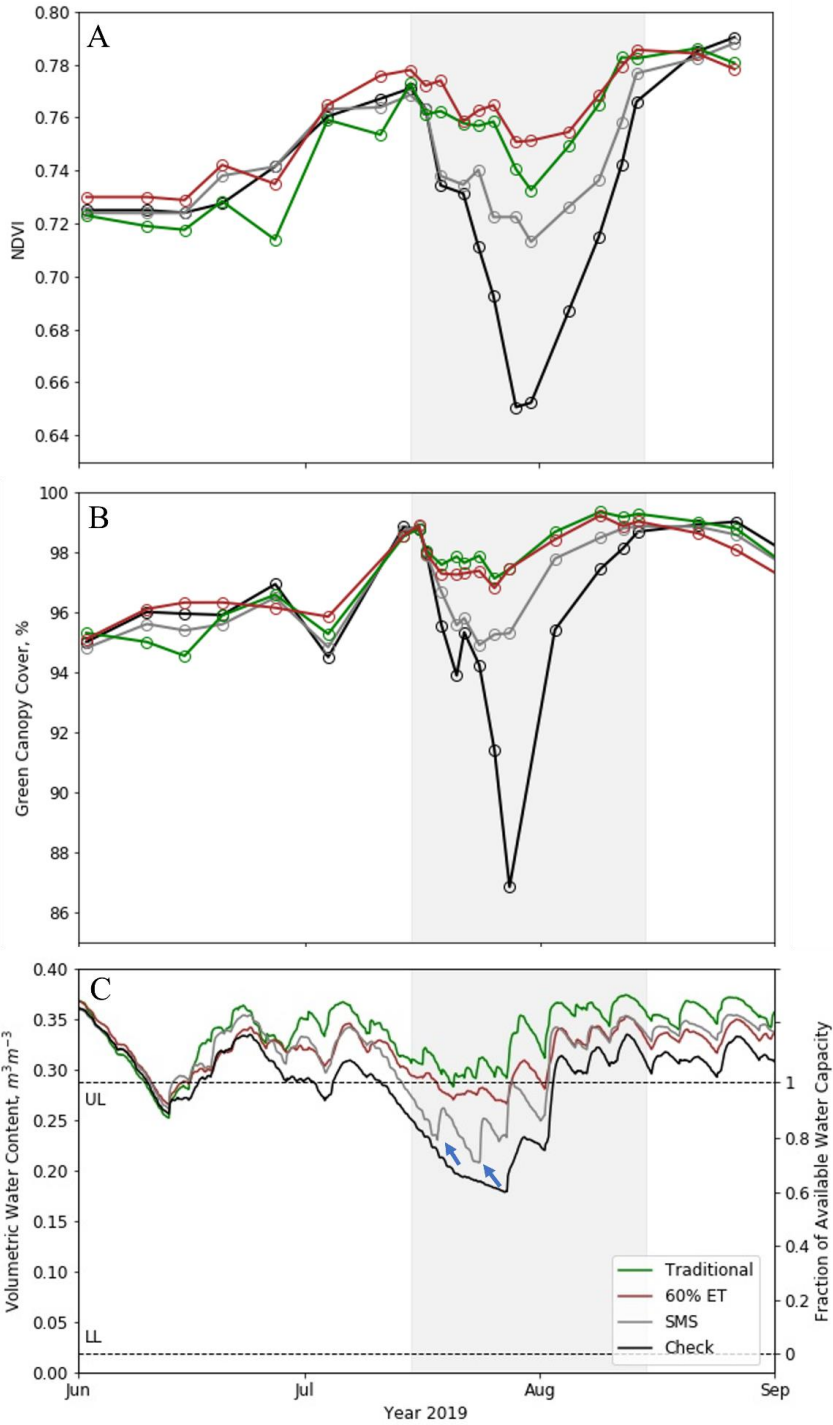
Figure 2.3 The relationship between normalized difference vegetation index (A), green canopy cover (B), and volumetric water content (C) for each treatment throughout the 2019 growing season. The dashed horizontal lines represent the upper limit (UL; 10% air-filled porosity) and lower limit (LL; permanent wilting point). The blue arrows indicate when irrigation was triggered in the SMS treatment. The shaded region highlights the decline and recovery of the canopy in the check treatment during a period of pronounced soil water deficit, spanning from 15-July to 15-August.
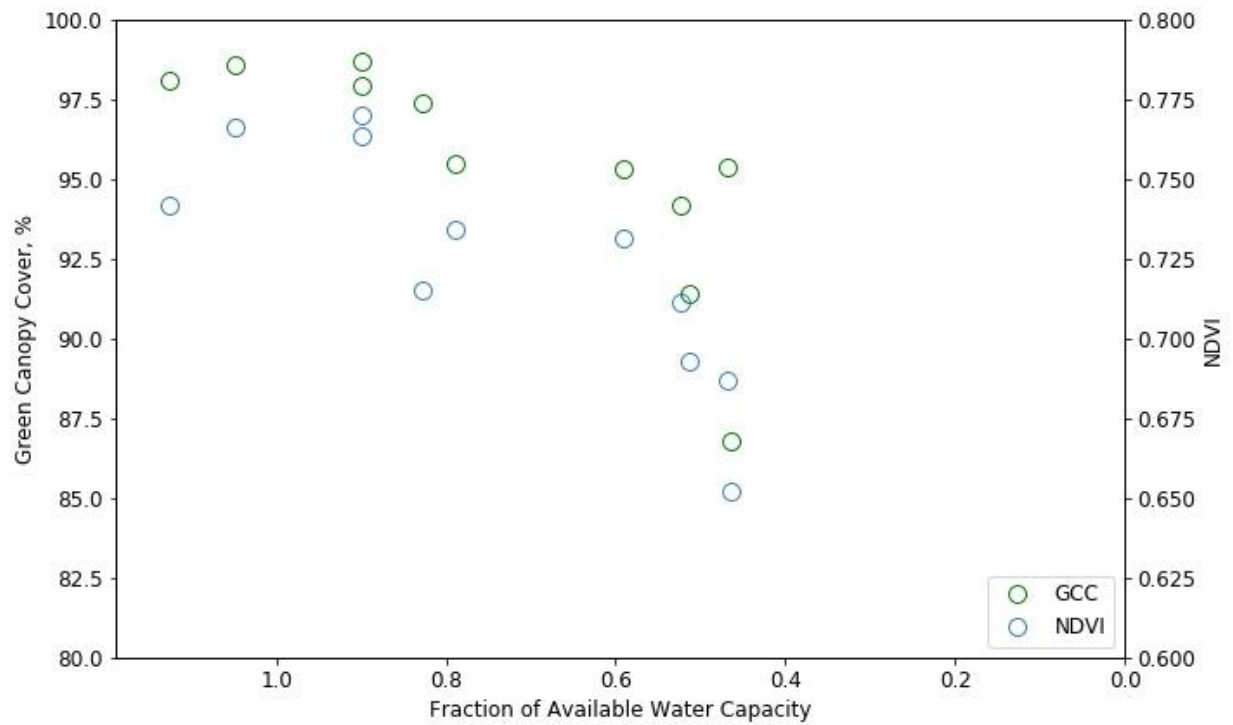
Figure 2.4 The relationship between GCC and NDVI as affected by the fraction of available water in the soil. Patterns of green canopy cover and NDVI illustrate the decline and recovery of the canopy in the check treatment (no irrigation) during and after a period of pronounced soil water deficit.
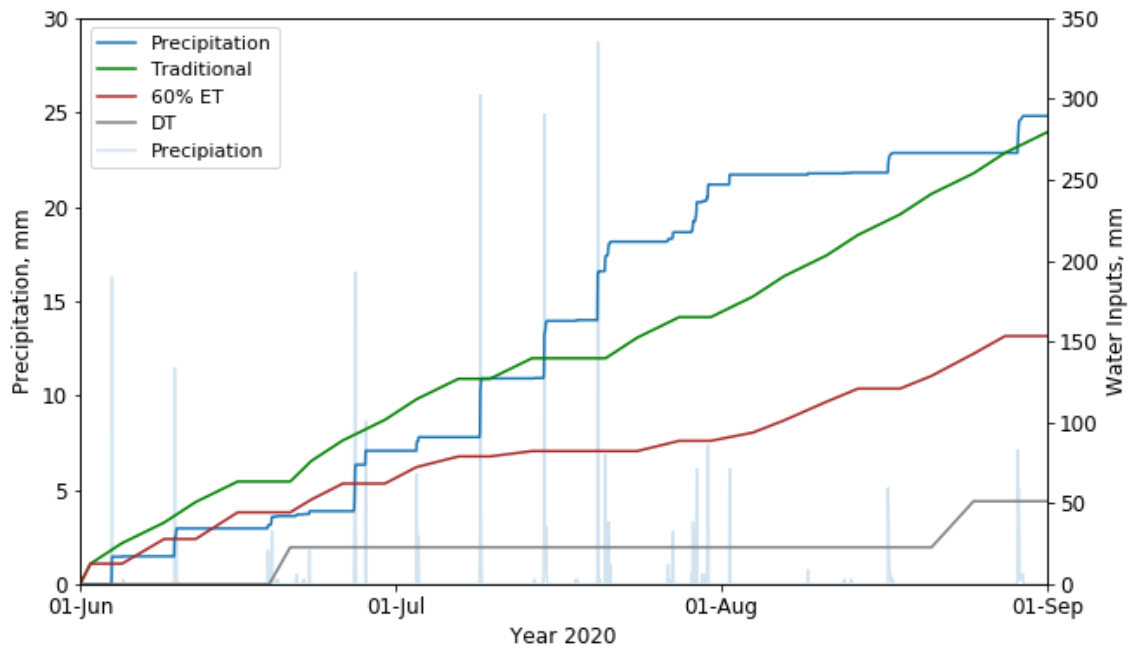
Figure 2.5 Daily precipitation and cumulative irrigation during the 2020 field study. Total precipitation was 286 mm, while irrigation water totaled 268 mm in the traditional treatment, 153 mm in the 60% ET treatment, and 51 mm in the DT-based treatment using the decision tree to guide irrigation events.
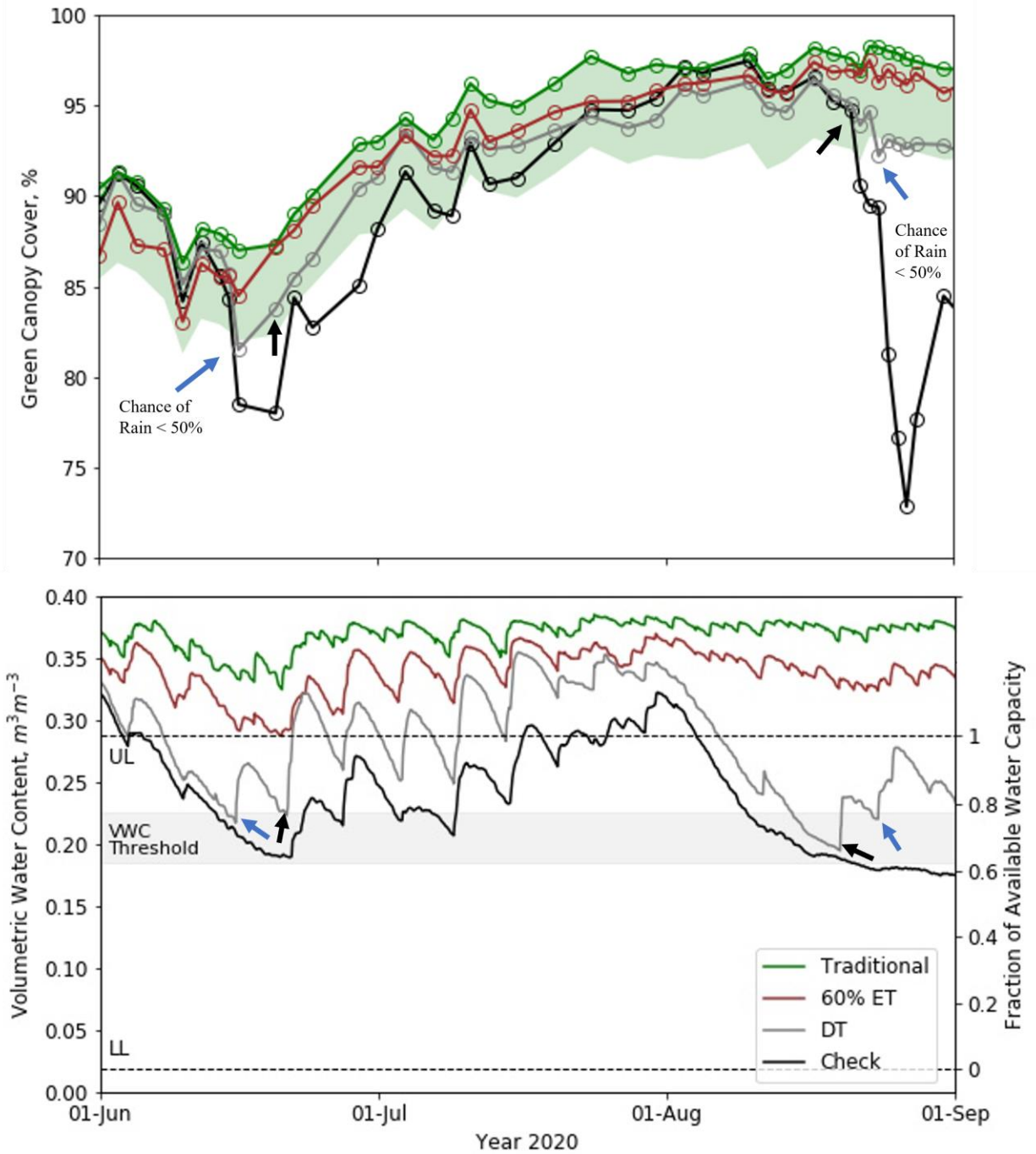
Figure 2.6 Components of soil-plant-atmosphere continuum through the 2020 growing season (volumetric soil water content, green canopy cover, forecast events). A) The shaded area in green canopy cover denotes the area 5% below the traditional irrigation treatment and the shaded area in volumetric soil water content denotes the threshold range for triggering irrigation. B) Four arrows depict dates when volumetric water content in the decision tree DT-based treatment reached the irrigation threshold. Two blue arrows indicate when irrigation was triggered for the DT-based treatment and two black arrows indicate GCC was still within the 5% range of the traditional treatment, bypassing the irrigation event.
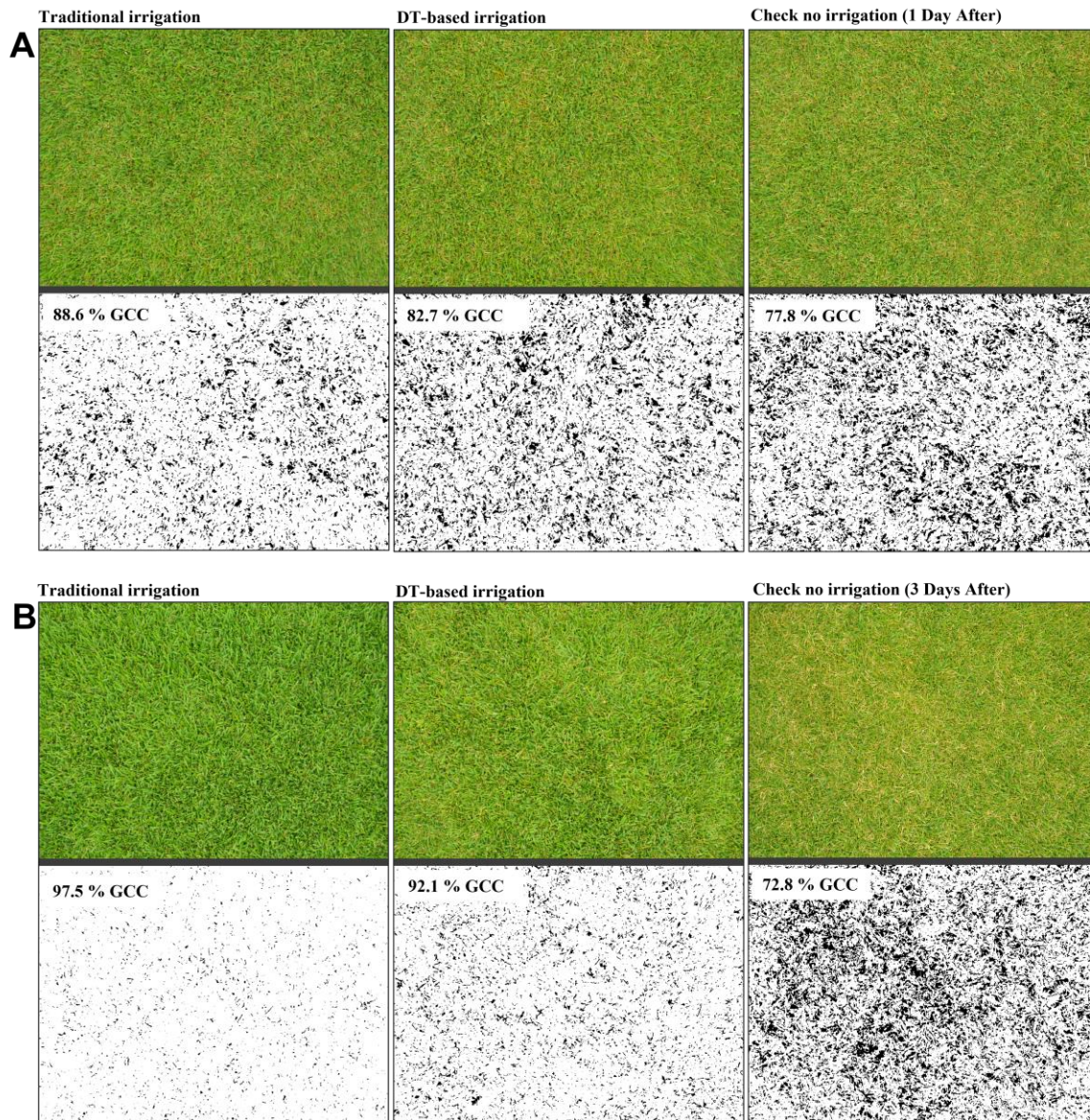
48

Figure 2.7 Green canopy cover percentages in the traditional (left) and DT-based irrigation plots (middle) at the time when irrigation was triggered based on the decision tree thresholds on (A) 20 July and (B) 24 August, 2020. The check treatment (right) illustrates the continued decline in green cover one and three days after irrigation was triggered on 20 July and 24 August, respectively, in the DT-based treatment. Green plant tissue is indicated by the white pixels.
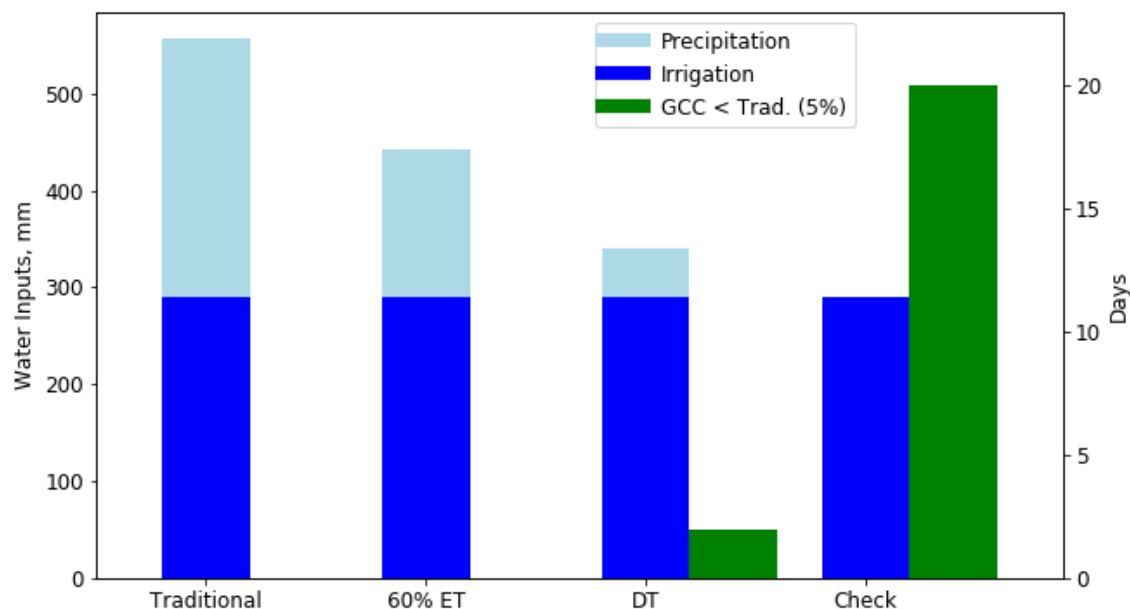
Figure 2.8 Total water inputs shown for each treatment from precipitation and irrigation. Green bars denote the total number of days when green canopy cover (GCC) in the DT and check irrigation treatments was >5% below GCC in the traditional irrigation treatment during 2020; GCC in 60% ET never fell more than 5% below the traditional irrigation treatment.
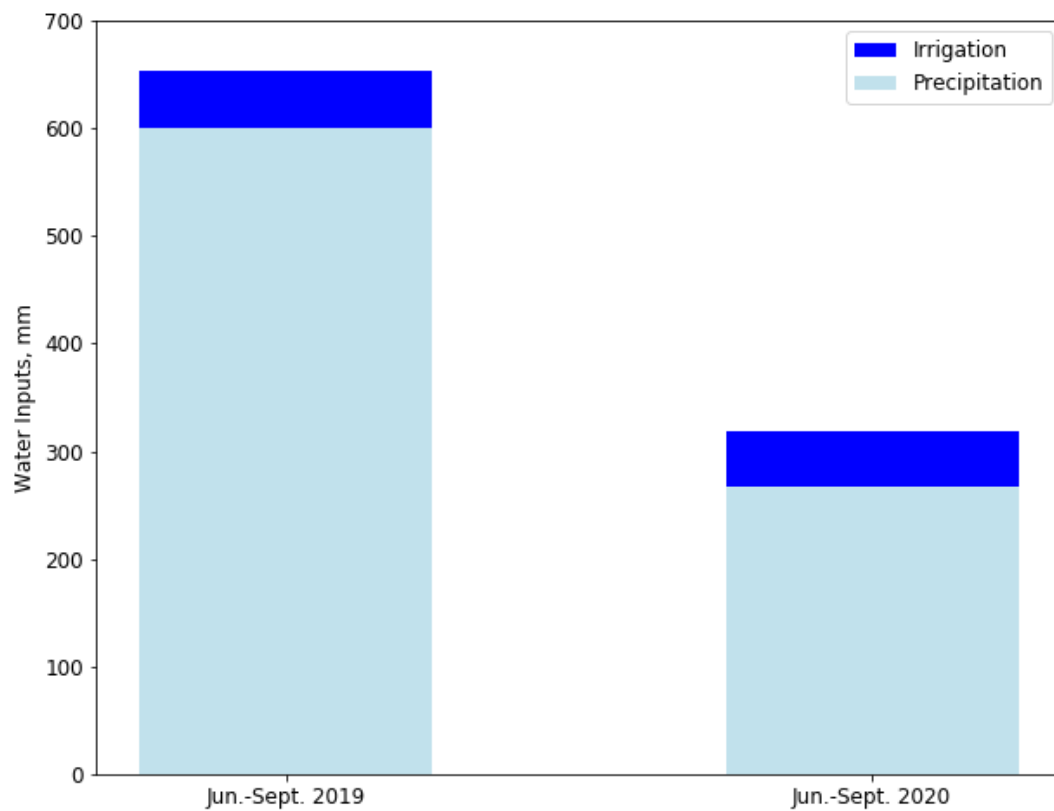
Figure 2.9 Total water inputs from irrigation and precipitation in the SMS treatment during 2019 and the DT-based treatment during 2020.

Table 2.1 Average annual precipitation (mm) over 30 years (1991-2020) and precipitation totals during the study in Manhattan, KS.

Year	June	July	August	Totals
30-yr avg	139	117	112	368
2019	175	152	274	601
2020	83	165	40	288

Appendix A - Pilot Experiment

Figure A. 1 Experimental design of the pilot experiment in the greenhouse using soil moisture sensors.
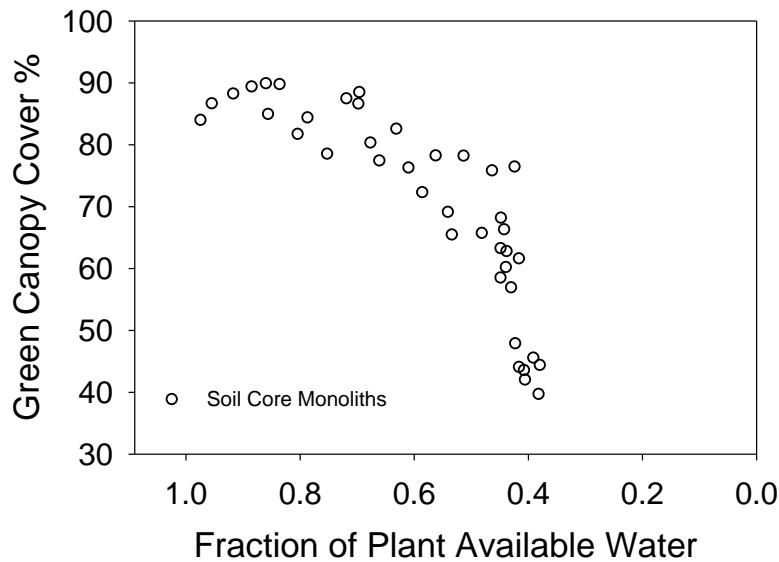
Figure A.2 Average relationship between green canopy cover and fraction of plant available water.

Prior to the field research, a pilot experiment was conducted on 'Meyer' zoysiagrass (Zoysia japonica L.) in the greenhouse to force a dry down period to monitor the turf canopy response to VWC. Four undisturbed soil core monoliths (20 cm diam. x 38 cm height) were taken from the research site and placed in PVC tubes. A time-lapse camera was mounted above the soil core monoliths to collect digital images every hour of the turf canopy. Soil moisture sensors (CS665, Campbell Scientific, Logan, Utah) were placed horizontally at a 10 cm depth to collect VWC. Air temperature and relative humidity sensors (CS215, Campbell Scientific, Logan, Utah) monitored atmospheric conditions within the greenhouse. Soil core monoliths were watered to field capacity, and a dry down period was enacted for 40 days. Results indicated a decrease in VWC by 15% (i.e., from 30% to 15%) during the dry down period, and green cover of the canopy decreased by 50% (i.e., from 92% to 42%). The onset of turf canopy stress was first detected at 0.70 fraction of plant available water.